MITOGEN ACTIVATED PROTEIN KINASE SIGNALING IN MOUSE SKELETAL MUSCLE

By

Natalie Maria Pizzimenti

A THESIS

Submitted to
Michigan State University
in partial fulfillment of the requirements
for the degree of

Physiology –Masters of Science

2014

ABSTRACT

MITOGEN ACTIVATED PROTEIN KINASE SIGNALING IN MOUSE SKELETAL MUSCLE

By

Natalie Maria Pizzimenti

AMP activated protein kinase (AMPK) and p38 mitogen activated protein kinases (MAPKs) are activated during exercise and thought to be involved in mitochondrial biogenesis through activation of PGC-1α. AMPK is activated through an increase in AMP (Hardie et al. 1998) however the activation mechanisms of the isoforms of p38 MAPK are currently unknown in skeletal muscle. It is hypothesized that exercise induced energetic drain induces phosphorylation of AMPK specifically leading to downstream phosphorylation of the p38γ MAPK isoform. Inhibitors of the two major ATPases suggest that energetic drain, not calcium cycling or force production, leads to the phosphorylation of p38γ MAPK. Direct activation of AMPK using AICAR revealed AMPK is insufficient to significantly activate p38γ MAPK. 2-deoxyglucose had no effect on the activation of either AMPK or p38γ MAPK. Further studies need to be conducted to determine the signaling pathway for activation of mitochondrial biogenesis.

To my loved ones.

ACKNOWLEDGMENTS

I would like to thank Dr. Bob Wiseman for guiding me through my master's research and always encouraging me to attain my full potential. I look forward to working more with him in the future. I would like to thank my committee members Dr. Ron Meyer, Dr. Jeff Brault, and Dr. Nara Parameswaran for their advice and assistance in this research presented. Finally, I would like to acknowledge the physiology staff and students who helped with furthering my education and helping me to become a better scientist.

TABLE OF CONTENTS

LIST OF TABLES

LIST OF FIGURES

KEY TO ABBREVIATIONS

MAPK	mitogen activated protein kinase
AMPK	AMPK activated protein kinase
PGC-1α	Peroxisome Proliferator-Activated Receptor Gamma Coactivator 1 Alpha
CPA	cyclopiazonic acid
BTS	N-benzyl-p-toluene
AICAR	5-Aminoimidazole-4-carboxamide ribonucleotide
DG	2-Deoxyglucose

INTRODUCTION

Exercise causes beneficial adaptations to the body by increasing its performance ability. One of these adaptations is an increase in aerobic capacity through mitochondrial biogenesis, increasing both the size and the number of mitochondria in the muscle. Currently, physiological aspects of exercise that initiates mitochondrial biogenesis are not well understood. In order to further gain understanding of the mitochondrial biogenesis signaling pathways, a basic understanding of skeletal muscle structure and function is needed.

Structure of Skeletal Muscle

Skeletal muscle is used in everyday activity and provides support via their connection to the skeleton by tendons. Every muscle fiber is bound together by the sarcolemma or the cell membrane of the muscle cells. Fibers are multinucleated, with the nuclei located along the outer edge of each cell. About 70% of the muscle cell mass is composed of the contractile unit or the myofibril. The myofibrils are composed of the sarcoplasmic reticulum and the transverse tubules. Myofibrils are arranged in repeating units termed the sarcomere, which extends from z-line to z-line (Elizabeth M. McNally, Karen A. Lapidos 2006) (Figure 1).

The thick and thin filaments are what allows the shortening of a skeletal muscle myofibril and allow force production. The thick filaments, multi-molecular aggregates of myosin, are connected to form the M-line. Myosin is composed of two heavy chains and four light chains. The thin filaments are composed of two chains of actin that intertwine in order to form an open double-stranded helix. The grooves of the helix have tropomyosin bound to troponin in the resting state of the muscle. When bound to tropomyosin, there is inhibition of the actin-induced stimulation of Magnesium-ATP hydrolysis. The thin filaments are anchored to the z-line, of

which were defined above as where each sarcomere begins and ends (McNally et al. 2006) (Figure 1).

Muscle Fiber Types

Myofibers can be classified into four different compositions based on their myosin heavy chain isoform. The compositions are: type I, type IIa, type IIb, and type IIx fibers. Type I and IIa use oxidative metabolism where types IIx and IIb are primarily glycolytic. Type I myofibres, or slow-twitch, are rich in mitochondria and have more capillaries surrounding each fiber. They have slow contraction with low shortening velocity, yet they have a higher resistance to fatigue. Slow-twitch oxidative fibers are typically postural muscles. Type IIa fibers, a fast-twitch phenotype, have a rapid shortening rate but fatigue more quickly than type I fibers. Both type IIx and IIb glycolytic fibres are capable of exerting a high amount of force over a shorter amount of time, but they fatigue quickly due to low vascularization and mitochondrial content (Bassel-Duby & Olson 2006).

There are also differences in the ryanodine parvalbumin and the sarcoplasmic reticulum calcium ATPase (SERCA) between the fiber types (Bassel-Duby & Olson 2006). Ryanodine receptors are channels on the sarcoplasmic reticulum that release calcium down its concentration gradient. Fast-twitch muscles have a faster acting ryanodine receptor (RYR1), which is what allows them to have a more rapid contraction time. SERCA is an ATPase which restores the calcium ions back into the sarcoplasmic reticulum (SR) in order to maintain the concentration gradient after contraction. Parvalbumin, in fast-twitch muscles in smaller mammals, is a protein that buffers calcium levels and shortens contraction time. Slow-twitch muscles have a longer contraction time due to their slower ryanodine receptors and SERCA subtypes. In addition, they do not have

parvalbumin to assist in the relaxation of the contraction through buffering the cytosolic calcium ions (Heizmann et al. 1982).

Contraction in Skeletal Muscle

Skeletal muscle contractions are occurring constantly to assist through the everyday tasks of life. A contraction begins with the activation of a motor unit by the central nervous system. Each motor unit innervates one or more skeletal muscle fibers. Motor unit recruitment happens sequentially (Fuglevand 2011). The size of the motor neuron is determined by the type of muscle it innervates. Slow fibers are innervated by small, slow conducting, low threshold units; whereas fast fibers are innervated by fast conducting, large units. The size of the motor unit determines the threshold of the neuron and its function (Henneman & Olson 1965). The final force production of the muscle is determined by which motor units were activated. Individual motor units are activated with an increase of sodium ions that cause depolarization of the neuron (MacIntosh & Shahi 2011). This depolarization, or action potential, travels down the length of the axon into the transverse tubules. The excitation spreads longitudinally along the sarcolemma and travels inwards toward each z-line by the transverse tubules, which are invaginations of the sarcolemma. Sodium floods the transverse tubules that are coupled to the sarcoplasmic reticulum by tight contact with the membrane and the terminal cisternae. The transverse tubules induce a conformational change to the dihydropyridine receptor (DHPR), a voltage-gated calcium channel. The DHPR cause an increase in permeability of the SR, via the ryanodine receptors, allowing calcium to flow out and flood the cytoplasm. The rise in the calcium concentration activates the troponin-inhibited contractile units on the thin filaments, allowing a conformational change that exposes the myosin binding site for the thick filaments. The myosin

heads are able to bind, hydrolyze ATP and shorten to produce force. This bond is broken once the myosin head binds another ATP molecule (MacIntosh & Shahi 2011; Huang et al. 2011). The actinomyosin ATPase is considered to be one of the two major ATPases in skeletal muscle during contraction (MacIntosh et al. 2012). There is successive activation of the sarcomeres in order to ensure that there is a wave of contraction that passes along the muscle. Sarcomeres cannot contract simultaneously due to their connecting z-lines, otherwise they would be pulled equally in opposite distances (McNally et al. 2006). Finally, the increase of calcium in the cytosol causes SERCA to be turned on and pump calcium back into the SR. SERCA is the other of the two major ATPases used during contraction, requiring ATP to pump calcium against its concentration gradient back into the SR. Once the cytosolic calcium concentration is at 10^{-7} M, all the calcium is back in the SR and stimulation ceases (MacIntosh et al. 2012).

Cell Signaling and Mitochondrial Biogenesis

Exercise has well known benefits that affect all organs in the body. It has shown to be beneficial in both states of health and disease. Some benefits of exercise include a reduced risk for cardiovascular disease, metabolic disorders such as Type II diabetes, hypertension, muscle, bone and joint disease, and depression (Vina et al. 2012). Normally in healthy muscle, modifications are occurring in a feedback loop in order to improve exercise performance. Some of the adaptations occurring in skeletal muscle include an increase in aerobic capacity, fiber-type transformation, increased sensitivity to insulin, and muscle hypertrophy (Vina et al. 2012).

The focus of this study is the signaling pathway for mitochondrial biogenesis which allows an increase in aerobic capacity (Booth et al. 2002). Peroxisome proliferator-activated receptor-(PPAR) co-activator 1α (PGC-1α) is a transcriptional co-activator that is a marker of mitochondrial biogenesis (Wu et al. 1999). PGC-1α, once activated, is trans-located into the

nucleus and induces activation of transcription factors such as mitochondrial transcription factor A (TFAM), and nuclear respiratory factor 1 (NRF-1) and 2 (Wu et al. 1999; Hoppeler & Fluck 2003). These signaling mechanisms leading to mitochondrial biogenesis are well described, yet what physiological aspect of exercise induces activation of PGC-1α is still unclear.

Signaling pathways associated with mitochondrial biogenesis and the activation of PGC-1α are calcium/calmodulin dependent kinase (CaMK) IV, force production, AMP activated protein kinase (AMPK), and p38 mitogen activated protein kinases (MAPK) (Chin 2004; Pogozelski et al. 2009; Winder et al. 2013; Csukly et al. 2002). An increase in intracellular calcium levels has been associated with mitochondrial biogenesis through PGC-1α, possibly through the CaMK pathway. Ojuka et al. show in L6 myotubes that by increasing levels of intracellular calcium with caffeine there is an increase in the expression of PGC-1α. Dantrolene treatment, which blocks calcium release from the sarcoplasmic reticulum, blunts the increase in the expression of PGC-1α (Ojuka et al. 2003). However, there were no other measurements of potential activation (such as energetic demand) in their study. Caffeine treatment causes calcium concentrations to be increased in the cytosol. Calcium will then bind to troponin causing a conformational change in actin and allowing myosin heads to bind. This has activated the actinomyosin ATPase. Along with the previous, SERCA will be turned on in order to pump calcium back into the SR. Therefore, the caffeine experiments did not isolate calcium signaling from energetic drain or from tension of the muscle cells. When calcium is not in the cytosol with the dantrolene experiments, there is neither activation of the actinomyosin ATPase nor the need for SERCA to be turned on to pump calcium back into the SR. These muscle cells are essentially in a resting state, and there is no change in the energetics. The energetic state of the myotubes was not taken

into consideration during these experiments and could have played a role in the expression levels of PGC-1α.

The p38 MAPK isoforms have been associated with PGC-1α and mitochondrial biogenesis via an increase in activation/phosphorylation with exercise (Puigserver et al. 2001; Akimoto et al. 2005). One of the mechanisms thought to induce activation of the of p38 MAPKs was force production (Csukly et al. 2002; Ryder 2000). Ryder et al. looked at muscle contraction independent of surrounding tissues or systemic factors. Rat epitrochlearis were incubated in tissue baths, and stimulated every 60 seconds for 10 minutes. Their results show that there is an increase in the activation of p38 MAPK (Ryder 2000). The Wiseman lab previously dissociated the connection between force production and the increase in phosphorylation/activation of the p38 MAPKs (Dentel et al. 2005). They show this by using N-benzyl-p-toluene (BTS), an inhibitor of the actinomyosin ATPase. BTS allows for calcium to still be released into the cytoplasm, but there is no force production. There is no change in the phosphorylation state of the p38 MAPKs with BTS during stimulation in comparison to control, suggesting force production is not the mechanism of activation (Dentel et al. 2005). The previous studies showing force production induces activation did not consider the other physiologic events that occur during contraction, such as calcium cycling, actinomyosin cross-bridge cycling, and energetic demand.

Finally, AMPK has been linked to mitochondrial biogenesis through PGC-1α (Jäger et al. 2007; Winder et al. 2013; Frier et al. 2012). Jäger et al. show in primary muscle cells that incubation with 5-Aminoimidazole-4-carboxamide ribonucleotide (AICAR), a synthetic activator of AMPK, causes an increase in PGC-1α mRNA and mitochondrial enzymes. They also make *in vivo* measurements with 6 hour incubations of AICAR injections in mice. This result shows an

increase in PGC-1α mRNA and cytochrome c expression suggesting mitochondrial biogenesis has occurred through activation of AMPK (Jäger et al. 2007).

Structure and Mechanisms of p38 MAPKs and AMPK

There are four isoforms of p38 MAPK expressed in skeletal muscle: α, β, γ, and δ (Hu 1999; Keesler et al. 1998). Each of the isoforms has distinct roles and respective locations throughout the body, with γ being most predominant in skeletal muscle (Cuenda & Rousseau 2007). The activation mechanisms of the p38 MAPKs is through dual phosphorylation of conserved Thr-Gly-Tyr (Cuadrado & Nebreda 2010). Selective activation of the isoforms of p38 MAPK can be done through formation of functional complexes between the isoforms and their upstream kinases, MAPK kinase-3, MAPK kinase-4, and MAPK kinase-6 (MKK3, MKK4, and MKK6) (Enslen et al. 2000; Keesler et al. 1998). MKK6 can phosphorylate all of the p38 isoforms, but MKK3 can only phosphorylate p38α and γ, not β. The p38 MAPKs become fully activated through dual phosphorylation at residues Thr180 and Tyr182, within the T-loop. Activation is dependent upon the kinase; MKK3 can phosphorylate only Thr180 whereas MKK6 phosphorylates both Thr180 and Tyr182 (Morrison & Davis 2003; Wang 1998).

AMPK is a heterotrimeric complex with an α catalytic subunit and two regulatory subunits, β and γ (Hardie et al. 1998). There are 12 different combinations of the complex, but there is one predominate configuration located in skeletal muscle which is composed of α_2, β_2, and γ_3 (Mahlapuu et al. 2004). AMP can activate AMPK through multiple mechanisms: allosteric binding to AMPK, allosteric binding to AMPKK, and binding to AMPK in order to make it a better substrate for AMPKK binding (Hardie et al. 1998). This is done through phosphorylation of the threonine residue 172. Binding of AMP to this residue inhibits phosphatase activity,

whereas high concentrations of ATP inhibit phosphorylation/activation of AMPK (Long & Zierath 2006).

In skeletal muscle, the activation site of AMPK for both exercise and AICAR is through the α_2 subunit (Jørgensen et al. 2004). This is shown by Jorgensen et al. through specific knockout mice of both the α_1 and α_2 subunit. With either electrical stimulation or incubation of AICAR, AMPK activation is ablated with the α_2 subunit knockout, but not the α_1 knockout. This suggests that both exercise and AICAR activate the same α isoform and through a similar mechanism.

Specific Aim I: Signaling Mechanisms of the p38 MAPKs

It was hypothesized that energetic stress induced through exercise leads to activation of the p38 MAPKs. To determine whether energetic stress has a role in activating the p38 MAPKs, the two major ATPases were inhibited individually and together. The two major ATPases in skeletal muscle, SERCA and actinomyosin, are responsible for about 97% of the energetic drain during contraction (MacIntosh et al. 2012). The inhibition of the actinomyosin ATPase by BTS, was shown to have no effect on the activation state of the p38 MAPKs (Dentel et al. 2005). With the use of CPA, an inhibitor of SERCA, calcium uptake is inhibited and high concentrations of calcium remain in the cytosol. This result will reveal if there is a connection to p38 MAPK activation and calcium cycling. The inhibitors in combination will inhibit the two major ATPases, which are responsible for about 97% of energetic drain in skeletal muscle during stimulation. This will test if energetic stress can induce activation of the p38 MAPK isoforms.

Specific Aim II: Inhibition of AMPK

If p38 MAPK is proven to be activated through an increase in energetic demand, then the next logical step would be to see if there is a correlation between AMPK and p38 MAPK. It was

hypothesized that inhibition of AMPK during stimulation would blunt phosphorylation of p38 MAPK. Compound c can be used to inhibit AMPK in rats during contraction (Funai & Cartee 2009). Once a dose response curve has been created to demonstrate that compound c functions in mouse skeletal muscle, than the inhibitor can be used to determine if AMPK can induce activation of p38 MAPK.

Specific Aim III: Synthetic Activation of AMPK

AICAR can be used in order to synthetically activate AMPK in a resting muscle (Corton et al. 1995); this is essential since there are no other contributing physiologic factors in question which normally occur during exercise. It was hypothesized that synthetic activation/phosphorylation of AMPK would lead to a downstream increase in activation/phosphorylation of p38 MAPK. Synthetic activation of AMPK would reveal if it alone is sufficient to activate p38 MAPK, all other events that happen during skeletal muscle contraction would not be factored into the equation.

Specific Aim IV: Isolation of Energetic Drain

If AMPK is not the direct activator of p38 MAPK, then energetics alone could be responsible for the activation of p38 MAPK. It was hypothesized that 2-deoxyglucose (DG), an inhibitor of glycolysis, would lead to an increase in energetic drain and induce phosphorylation of both AMPK and p38 MAPK. DG would isolate energetic stress from other physiological factors in skeletal muscle, and identify whether it alone is sufficient for the activation of p38 MAPK.

Each of these studies will contribute to furthering the understanding of the roles AMPK and p38 MAPK play in the signaling pathway for mitochondrial biogenesis.

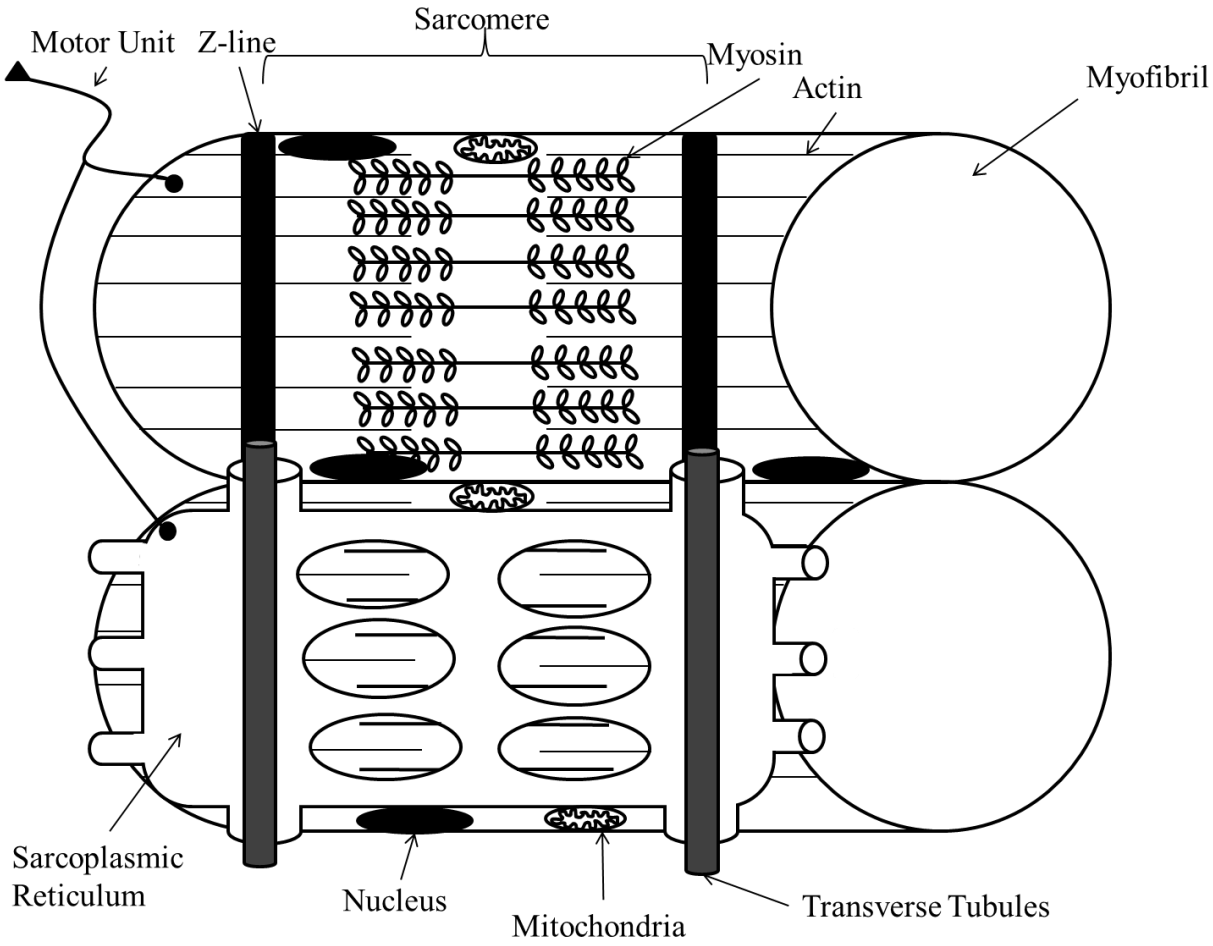

Figure 1. Myofibril Structure. Myofibrils are composed of repeating units of sarcomeres with peripheral nuclei. Excitation-contraction coupling begins with stimulation of the motor neuron. This action potential travels down the axon of the motor neurons to depolarize the transverse tubules. The transverse tubules, which are coupled to the SR, cause the release of calcium into the cytosol. Calcium binds to troponin and allows the conformational change of actin so the myosin head can bind inducing shortening of the muscle and force production. Skeletal muscle has peripherally located nuclei and mitochondria. The Z lines anchor the sarcomere to the plasma membrane.

MATERIALS AND METHODS

Materials and Animals

Adult, male Swiss Webster mice (28-32 g body weight) (Harlan, Indianapolis, IN) were housed in a 12h light/12h dark cycle and given food and water ad libitum. All protocols were approved by the Institutional Animal Care and Use Committee at Michigan State University (04/11-077-00).

ATPase inhibitors, N-benzyl-p-toluene sulphonamide (BTS) and cyclopiazonic acid (CPA) were purchased from Sigma-Aldrich Chemical Company (St. Louis, MO). Compound c, an AMPK inhibitor, was purchased from Sigma-Aldrich (St. Louis, MO; P5499). 5-Aminoimidazole-4-carboxamide-1-β-D-ribofuranoside, (AICAR) a synthetic activator of AMPK, was purchased from Toronto Research Chemicals (Toronto, Ontario; A611700). Rabbit polyclonal antibody to phosphorylated p38 (Thr180/Tyr182) was purchased from Cell Signaling Technology (Beverly, MA; catalog #9211). This antibody detects phospho-p38α, p38β, and p38γ isoforms. Total p38 was detected with rabbit antibodies specific for the α, β, and γ isoform (Cell Signaling Technology; catalog #9212). Goat anti-rabbit IgG linked to horseradish peroxidase was purchased from Cell Signaling Technology (catalog #7074). Rabbit polyclonal antibody to phosphorylated AMPKα (Thr172) was purchased from Cell Signaling Technology (Cell Signaling Technology; catalog #2535). This antibody detects both α-1 and α-2 isoforms. Total AMPK was detected with rabbit antibodies specific for the α isoforms (Cell Signaling Technology; #2532). Rabbit polyclonal antibody to phosphorylated ACC (Ser79) was purchased from Cell Signaling Technology (Cell Signaling Technology; #3661). This antibody detects both ACCα and ACCβ. Total ACC was detected with rabbit antibodies specific for all isoforms

of ACC (Cell Signaling Technology; #3662). Goat anti-rabbit IgG linked to horseradish peroxidase was purchased from Cell Signaling Technology (catalog #7074). All other chemicals were obtained from Sigma-Aldrich.

Isolated Muscle Preparations

Mice were anesthetized with an intra-peritoneal injection of pentobarbital (50 mg/kg). Extensor digitorum longus (EDL) muscles were ligated at the proximal and distal tendons with 5.0 silk sutures, removed from the hindlimbs, and secured in a 37°C water-jacketed organ bath (Radnoti Glass Technology, Inc., Monrovia, CA) at their approximate *in vivo* resting length. These mouse muscles have a small diameter allowing sufficient oxygen diffusion to the muscle core to maintain the proper energetic state (Crow & Kushmerick 1982; Robert W. Wiseman and Martin J. Kushmerick 1995). The bath contained 8 ml modified Ringer solution (117 mM NaCl, 4.6 mM KCl, 25 mM $NaHCO_3$, 2.5 mM CaC_{12}, 1.16 mM $MgSO_4$, and 11 mM glucose, pH 7.4) with 10 mg/L gentamycin and was continuously gassed with 95% O_2/5% CO_2.

Mice were euthanized via cervical dislocation. Muscles were field-stimulated via platinum electrodes using a Grass S88 Stimulator (Grass Instruments, Quincy, MA). After adjusting the muscle to optimal length (Lo) using the length tension relationship, initial maximal twitch force was determined using supramaximal voltage. Only muscles that were physiologically stable and able to generate 5 or more grams of force under supramaximal stimulation prior to the start of any experimental protocol were included in this study.

In the first study, muscles were treated with inhibitors and/or vehicle for a total of 60 minutes. To inhibit both cytosolic ATPases, muscles were first treated with BTS (in 20 µl DMSO). Thirty minutes later, CPA was added (in 20 µl DMSO). Muscles were treated in this order because

CPA causes a rise in intracellular calcium levels (Baudet et al. 1993; Robin et al. 2012) that may be sufficient to increase basal tension by activation of actomyosin ATPase. For experiments with a single ATPase inhibited, 20 µl DMSO was added to the bath during the first 30 minute period, followed by addition of either 20 µl BTS or CPA stock solutions for the remaining 30 minutes. The final concentration of DMSO was 0.5% (v/v) in all experiments. When present, the final concentration of BTS was 75 µM, and CPA was 50 µM.

Inhibitor concentrations were selected based on the minimum concentration sufficient to abolish the physiologic function of each ATPase. Dentel et al. have previously shown that 75 µM BTS is sufficient to inhibit force production by over 95% within 30 minutes with no effects on Ca^{2+} kinetics (Dentel et al. 2005). Using an increase in the relaxation time as an index of SERCA function, a similar dose response curve was generated for CPA to determine the optimal concentration to inhibit its function. Muscles were incubated in varying concentrations of CPA, and twitches were performed every 10 minutes for a 30 minute period.

Muscles were electrically stimulated with 0.5 msec duration pulses delivered at 10 Hz for 15 minutes. A small group of muscles were kept at Lo for the same duration (15 minutes) for non-stimulated resting controls. Immediately after the stimulation period, the sutures securing the muscles were cut, muscles rapidly blotted of to remove excess media and freeze-clamped between liquid nitrogen temperature stainless steel tongs to preserve the energetic state and protein phosphorylation status. Muscles were stored at -80°C until further analysis.

In the next series of experiment, all muscles were hung in the same manner as stated above. To determine the proper concentration of compound c necessary to inhibit AMPK, a dose response curve was generated using increasing concentrations (80, 100, 120 or 140µM) for 60 minutes

(Figure 5). After incubation with increasing concentrations of either compound c or the vehicle (DMSO), muscles were stimulated at 2 Hz for 20 minutes with a 2 ms pulse duration (Funai & Cartee 2009). Tendon-free EDLs weights were found before flash frozen and stored at -80°C until further analysis.

In order to test muscles with activated AMPK, muscles were hung at resting length and treated with 2mM AICAR (a synthetic activator of AMPK) or vehicle (DMSO) for 120mins. A twitch was performed every 30 minutes to each of the muscles in order to ensure that force was maintained over the incubation period. Tendon-free EDLs weights were found before muscles were flash frozen and stored at -80°C until further analysis was done.

In the final study, all muscles were hung at resting length and treated with either 20mM 2-deoxyglucose (DG) or vehicle (DMSO) for 40 minutes. Incubation with DG allows the isolation of energetic demand and the determination of its role in activation of p38γ MAPK. Twitches were administered every 10 minutes to ensure the viability of the muscle. Muscles were flash frozen and stored at -80°C until further analysis was done.

Metabolite Analyses

EDL muscles were cut free of their sutures on a liquid nitrogen cooled aluminum block and weighed while still frozen in order to maintain the metabolic state. Metabolites were extracted in 20 to 30-fold excess ice-cold 0.5 N perchloric acid with rapid homogenization by pre-cooled 1.4 mm stainless steel beads in a Bullet Blender (Next Advance). Extracts were neutralized and perchlorate was removed by the addition of ice-cold KOH and subsequent centrifugation at 4°C. Samples were stored at -80°C until analysis.

Concentrations of phosphocreatine (PCr), creatine (Cr), adenine nucleotides (ATP, ADP, and AMP), and adenine nucleotide degradation products (IMP, adenosine, adenine, and inosine) were determined by ultra performance liquid chromatography (UPLC) using a Waters Acquity UPLC H-class system. The method is based on a high performance liquid chromatography method from Teerlink et al. (Teerlink et al. 1993). UPLC separation was achieved by gradient reverse-phase chromatography using an Acquity UPLC HSS T3 1.8 µm, 2.1 x 150 mm column (Waters) maintained at 35°C. Mobile phases consisted of 0.2 M KH_2PO_4 (buffer A) and 50% water / 25% acetonitrile / 25% methanol (buffer B). Flow rate was a constant 0.4 ml /min with the initial conditions 98.5% buffer A and the balance buffer B. Starting at 0.1 minutes, the percent buffer A decreased linearly to 85% at 6 minutes and further decreased to 50% at 7 minutes. The mobile phase was returned to the initial buffer A: buffer B ratio (98.5: 1.5) at 7.2 minutes, where it remained until 10.5 minutes to re-equilibrate the column, after which a new sample could be injected. Metabolites were identified by comparison of peak retention times of pure, commercially available standards (Sigma-Aldrich), which were separated with baseline resolution in less than 7 minutes (Figure 6A). Baseline resolution was also achieved with extracts from non-contracted (Figure 6B) and 15 minute contracted (Figure 6C) EDL muscles demonstrating that other metabolites did not interfere with this chromatography method. Quantification was by comparing peak area at 210 nm, which was linear with amount injected from 0.2 pmol to 100 pmol with an r2 >0.998 for all metabolites.

Western Blot Analysis

Frozen muscles were homogenized in isotonic saline containing glycerol, DTT, SDS, protease inhibitors, and phosphatase inhibitors as previously described (Dentel et al. 2005). Briefly, 25 µg of total protein for each sample was resolved by sodium dodecyl sulfate polyacrylamide

electrophoresis (SDS-PAGE) through 10%, 12% acrylamide gels, or gradient gel (Bio-Rad) (w/v) acrylamide gels and then transferred onto nitrocellulose membranes. Gel was Coomassie stained and membranes were reversibly stained with Ponceau S to ensure equal loading and transfer of proteins. Membranes were blocked in 5% BSA in TBST or 5% Non-fat milk in TBST, then incubated overnight at 4°C with primary antibodies diluted 1:1000. After incubation with secondary antibody-HRP conjugate (1:2000), bound second antibody was detected using the Phototope-HRP Western Blot Chemiluminescent kit (Cell Signaling Technology, Beverly, MA). Chemiluminescent signals were visualized on Amersham ECL Hyperfilm (Amersham Biosciences, Piscataway, NJ), digitally captured, (EDAS 290 gel documentation system, Eastman Kodak, Rochester, NY), and quantified by densitometry (Quantity One Image Analysis software, BioRad, Hercules, CA). The amount of enzyme that is in the phosphorylated state for each p38 MAP kinase isoform was expressed as a ratio to the percent change from the control group for each protein used.

Statistics

Data are presented as the mean ± standard error (SE). Statistical significance ($P < 0.05$) was determined by ANOVA, followed by Tukey-Kramer HSD were appropriate.

A.

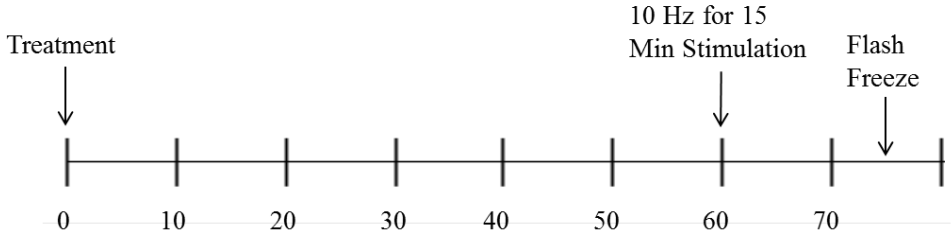

B.

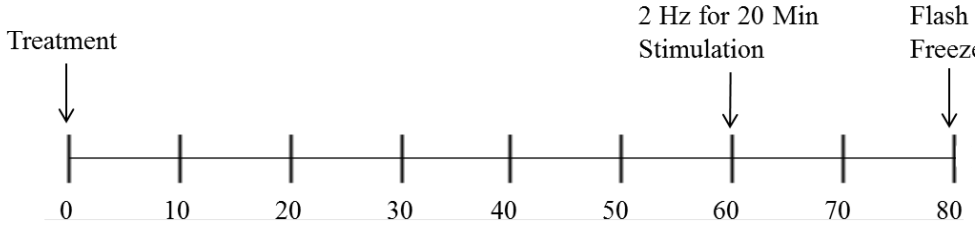

C.

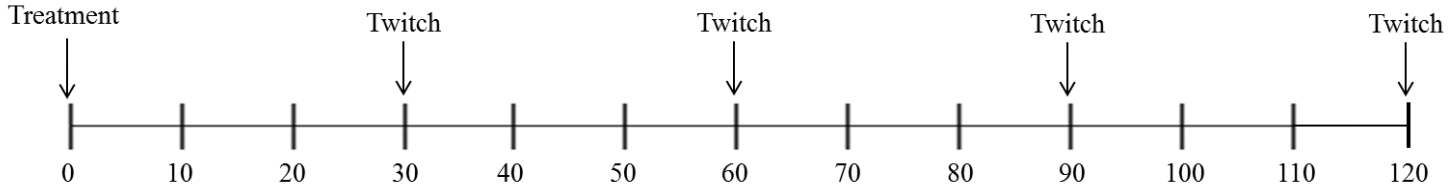

D.

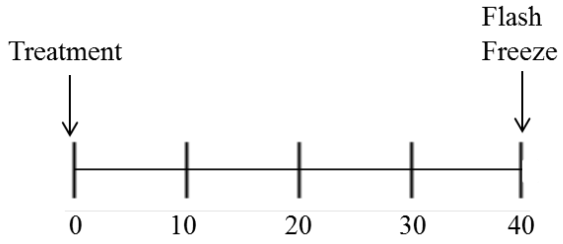

Figure 2. Treatment Timelines.

Figure 2 (cont'd). A. Specific Aim I. Timeline representation of the EDL treatment with either BTS, CPA, or BTS + CPA (Treatment) prior to stimulation at 10 Hz for 15 minutes. At the end of the stimulation, muscles were weighed and flash frozen before stored at -80°C until further analysis. **B. Specific Aim II.** Timeline representation of compound c (Treatment) incubation for 60 minutes prior to stimulation at 2 Hz for 20 minutes. Muscles were weighed, flash frozen and stored at -80°C until further analysis. **C. Specific Aim III.** Timeline representation of AICAR (Treatment) incubation for 120 minutes. A twitch was administered every 30 minutes in order to ensure the viability of the muscle. At the end of the incubation, muscles were weighed, flash frozen and stored at -80°C until further analysis. **D. Specific Aim IV.** Timeline representation of DG incubation for 40 minutes. At the end of the stimulation, muscles were weighed and flash frozen before stored at -80°C until further analysis.

RESULTS

Specific Aim I: Signaling Mechanisms of the p38 MAPKs

Inhibition of SERCA by CPA

Optimal concentration of CPA to inhibit SERCA function was derived from inhibitor titration experiments. All concentrations had a time-dependent increase in total relaxation time, reaching the maximum at 30 minutes (Figure 2). The highest concentration of CPA (250μM) had a decrease in peak force production (data not shown). Therefore, further CPA incubation experiments were done using 50μM concentrations in order to minimize the physiological effects seen on force production.

Specific Inhibitor Effects on Contractile Performance

Single twitch characteristics were analyzed both pre- and post-treatment (Table I) in order to discern the effects of each inhibitor alone or in combination on physiologic function. Control treatment (DMSO) in EDL muscles had no effect on twitch kinetics (Figure 4). BTS, an inhibitor of the actinomyosin ATPase, lead to >95% reduction in twitch peak force and the tension time integral. There was only a modest increase in rise time and decrease in relaxation time; this is consistent with observations reported previously from this laboratory (Dentel et al. 2005) and others (Cheung et al. 2002; Young et al. 2003). Incubation with CPA, a SERCA inhibitor, caused a 1.8-fold increase in peak force and seven-fold increase in the total relaxation time from 28 to almost 200ms (Table I). This is consistent with previous reports (Kurebayashi 1991; Même et al. 1998). There was a 12-fold increase in the tension-time integral for a single twitch, which would be due to both the increase in peak force and the longer relaxation time.

BTS+CPA in combination had little effect on twitch kinetics but force was decreased by >90%, most likely due to BTS which also contributed to the 90% reduction in the tension-time integral.

To look at the effect of the inhibitors on the function of the ATPases, the EDLs were stimulated at 10 Hz for 15 minutes. Control (DMSO) stimulated EDLs had force potentiation during the first few seconds to generate peak force values of almost 14grams. Force fell rapidly by 80% within the first four minutes of stimulation and remained at that level until the end of the stimulation protocol (Figure 5). The cumulative tension time integral, having an average of 127 N.s/gww, was used as an indication of the imposed workload. Treatment with BTS alone had a decrease in overall force production by 85%. The cumulative tension time integral for BTS-treated muscles was 20 N.s/gww. Peak force production was increased to over 28 grams in the stimulated CPA treated muscles. This was due to the inhibition of the calcium reuptake, but there was a rapid decrease of force within two minutes. There was failure of the EDLs to fully relax between pulses most likely due to the inhibition of the calcium re-uptake from the cytosol by SERCA; the stimulation protocol appeared as if it was one fused contraction (Figure 5). The cumulative tension time integral of the CPA treated muscles was 395 N.s/gww, which was the largest of all the groups. Similar to the BTS treatment alone, there was almost total loss of force production with the combination treatment of BTS and CPA. There was also an increase in relaxation time for each individual twitch and the cumulative tension-time integral was 35 N.s/gww.

HPLC

Consistent with previous HPLC measurements from perchloric acid extracts of the non-stimulated muscles (DMSO), the PCr/Cr ratio was approximately 3:1 (Table II) (Hancock et al.

2005; Kushmerick et al. 1992; Wiseman and Kushmerick 1995). This indicates that neither muscle incubation nor the treatment with DMSO have any detrimental effects on energetic state of the muscle. Inosine monophosphate levels, an indicator of long-term energetic drain, were 0.35 ± 0.09 μmol/gww, which is comparable to values reported by others in resting fast-twitch muscles from mice (Hancock et al. 2005).

A 73% decrease in both PCr and ATP concentrations ($p<0.05$) was seen in vehicle treated (DMSO) stimulated EDLs. Also, a concurrent 2.7-fold increase in Cr and a 7.1-fold increase in IMP ($p<0.05$) was seen (Table II). Stimulation also caused a slight, but significant ($P< 0.05$) increase in inosine concentration. However, both the adenine (0.12 μmol/gww) and the adenosine nucleotide pool (0.10 μmol/gww) were conserved over the course of the stimulation protocol. BTS treatment alone, causing inhibition of the actinomyosin ATPase, had no significant effect on the levels of PCr or ATP, and IMP accumulation was nearly identical to that of the control stimulated muscles (1.90± 0.09 μmol/gww). This indicates that the energetic costs of calcium handling are still consuming ATP within the 15 minute stimulation protocol. CPA treatment alone, causing inhibition of SERCA, with stimulation resulted in a decrease in PCr and ATP, but the accumulation of IMP was similar to that of the stimulated control EDLs (2.15± 0.21 μmol/gww). This indicates that there is still energetic demand occurring with SERCA inhibition, which could be due to the increased myosin ATPase use which is seen with the potentiation in force production (Table II and Figure 5). The combined treatment of BTS+CPA caused PCr, Cr, and ATP to be close to resting levels and only a modest decrease in the PCr/Cr ratio (Table 2). Most importantly, the IMP concentration (0.58 ± 0.08 μmol/gww) was not different than levels found in control non-stimulated muscles.

Phosphorylation of MAPK Isoforms by Western Blot Analysis

Stimulation at 10 Hz for 15 min profoundly increased the phosphorylation of the p38 isoforms in comparison to resting levels. Phosphorylated p38γ levels were increased by 3.44±0.26, and p-p38α/β was increased by 2.62±0.04 (n=3; p=0.001; p=6.4e-5) (Figure 7).

To test whether the phosphorylation state of the p38 isoforms were dependent on force production, muscles were incubated in the absence or presence of BTS, an actinomyosin ATPase inhibitor, and then electrically stimulated. Even with a dramatic decrease in force (Table I), BTS did not decrease the phosphorylation of the p38 isoforms as compared to control-stimulated muscles (Figure 8).

Sarcoplasmic reticulum-ATPase (SERCA) catalyzes the reuptake of Ca^{2+} into the SR, which can account for about 30% of the energetics used in contracting muscle (Rall 2005). To test if an increase in calcium in the cytosol or the energetic cost of the reuptake of Ca^{2+} induces phosphorylation of the p38 isoforms, muscles were treated with CPA. In stimulated CPA treated muscles, the phosphorylation pattern for the p38 isoforms was not significantly different from the control-stimulated muscles (Figure 9).

Treatment with both BTS and CPA, inhibits the two major ATPases and causes energetic drain during contraction to be reduced by about 95%. In stimulated muscles treated with both BTS and CPA (Figure 10), the phosphorylation of p38 α/β (0.85± 0.77) was no different from muscles treated with BTS alone (1.0± 0.10). However, the phosphorylation of p38γ was significantly blunted (0.45± 0.67)(n=4; p=0.04) in comparison to BTS-treated muscles (1± 0.16).

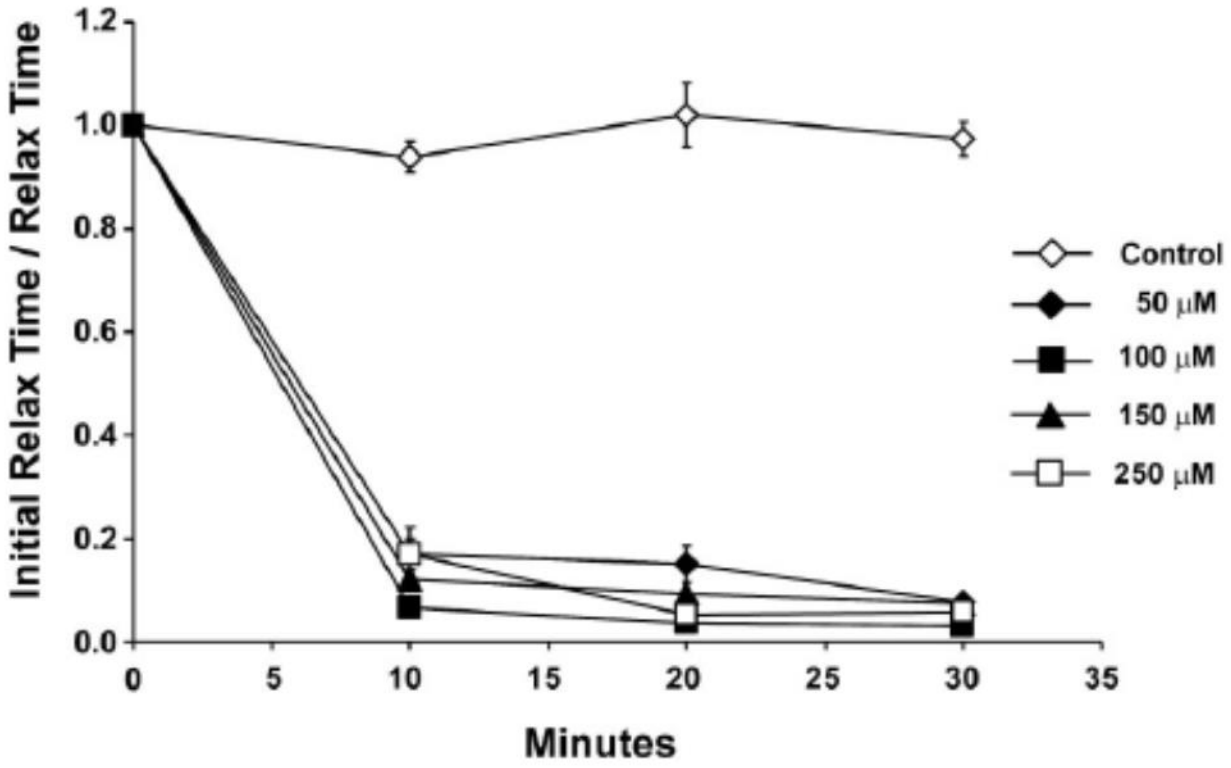

Figure 3. CPA Dose Response Curve. Dose response curve for cyclopiazonic acid (CPA) over time in isolated EDL mouse muscles incubated at 4 different concentrations. Inhibition of SERCA by CPA was evaluated by measuring the total relaxation time for each contraction (in msec) and normalized to the percent of initial then expressed as the reciprocal. The data are presented as mean ± SEM.

Table I. Muscle Twitch Characteristics. Muscle mass and twitch characteristics before (Pre-Treatment) and after (Post-Treatment) treatment with DMSO (control), 75µM BTS, 50µM CPA, and BTS+CPA.

		Pretreatment				Posttreatment			
	Weight (mg)	Rise time (ms)	Relaxation time (ms)	Peak force (N/g)	TTI (N s/g)	Rise time (ms)	Relaxation time (ms)	Peak force (N/g)	TTI (N s/g)
Control	10.3 ± 0.5	10.0 ± 0.3	20 ± 3	12.0 ± 1.0	0.15 ± 0.01	10.0 ± 0.0	19 ± 0	10.8 ± 0.7	0.165 ± 0.013
BTS	10.3 ± 0.3	11.2 ± 0.5	28 ± 4	8.5 ± 0.4	0.12 ± 0.01	8.5 ± 1.4	18 ± 1	0.6 ± 0.2	0.006 ± 0.002
CPA	7.8 ± 0.3	9.3 ± 0.7	28 ± 4	8.5 ± 0.9	1.14 ± 0.01	28.7 ± 3.7	198 ± 165	15.5 ± 1.4	2.045 ± 0.345
BTS + CPA	13.8 ± 1.0	12.0 ± 0.9	30 ± 8	6.6 ± 0.5	0.15 ± 0.03	11.7 ± 1.3	30 ± 8	0.3 ± 0.03	0.017 ± 0.003

The values represent the average rise time, relaxation time, peak force, and tension time integral ± SE (n = 6 or 7 per group).

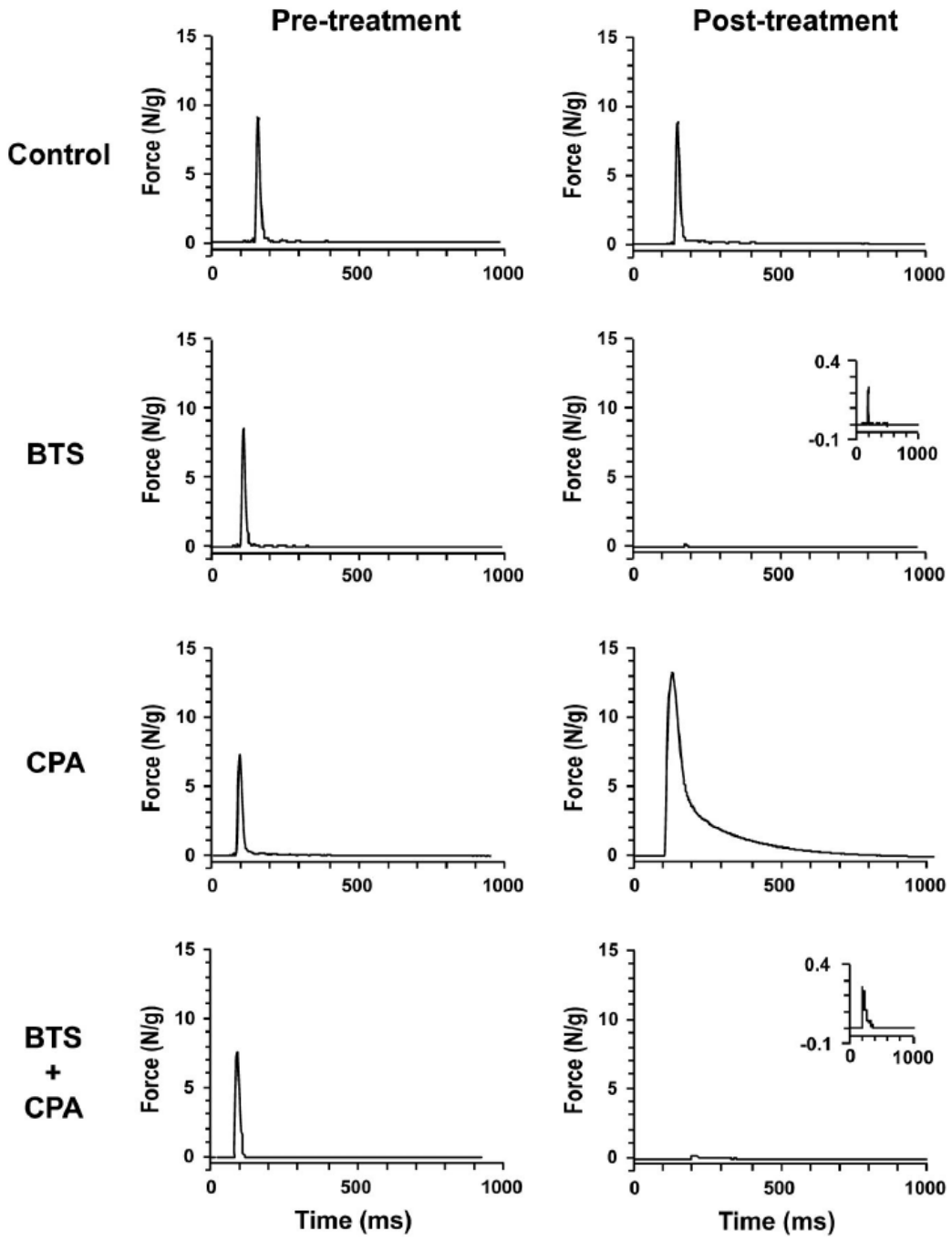

Figure 4. Treatment Effects on Twitch Characteristics. Representative twitch force recordings of electrically stimulated muscles before (Pre-) and after (Post-) treatment with DMSO (Control) or with the ATPase inhibitors BTS (75 µM), CPA (50 µM), and CPA (50 µM) + BTS (75 µM).

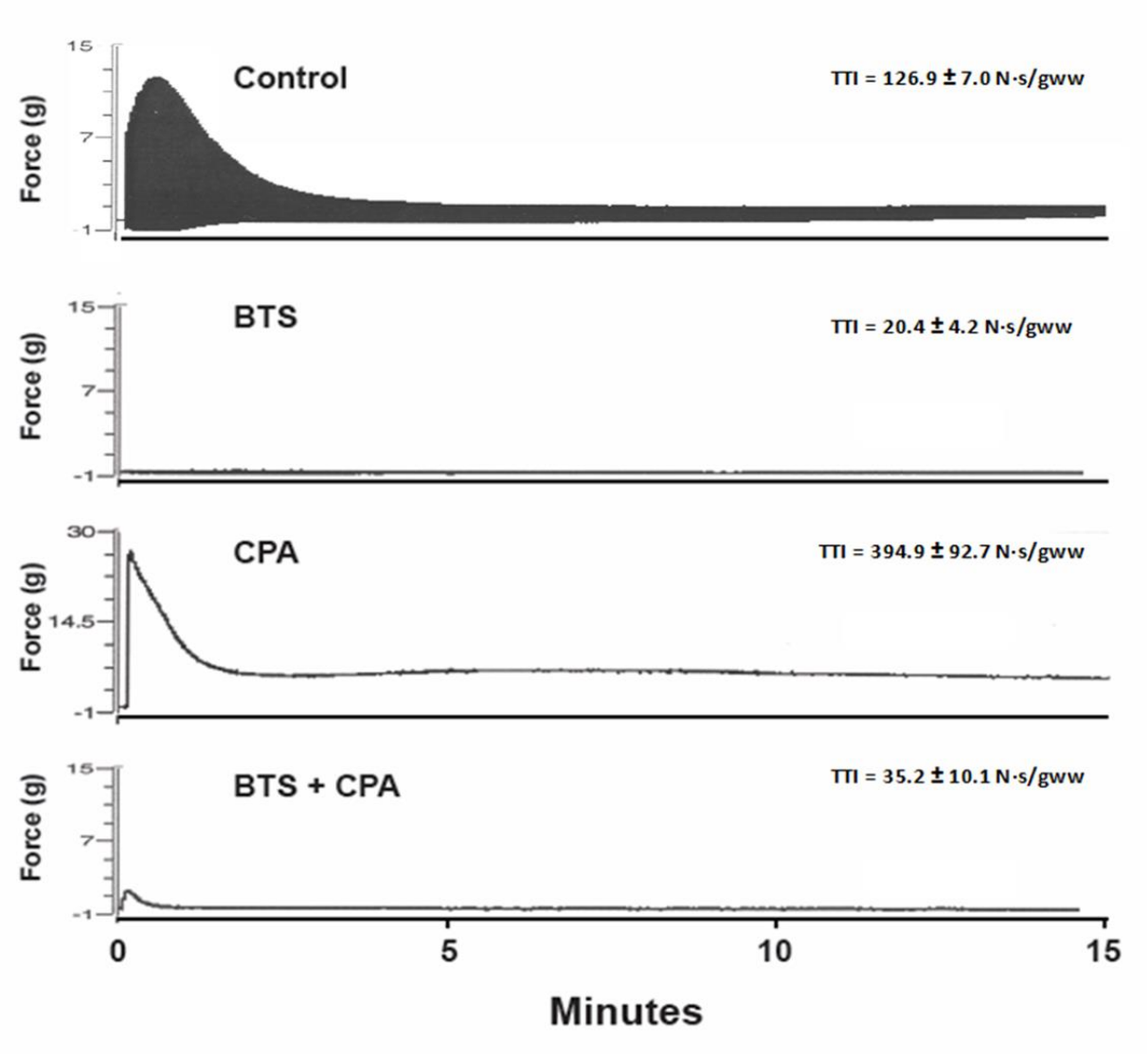

Figure 5. Treatment Effects on Fatigue Protocol. Representative force recordings of incubated muscles electrically stimulated at 10 Hz for 15 min. Muscles were treated with DMSO (control) (n=6), BTS (n=7), CPA (n=7), or CPA + BTS (n=7) for 60 minutes before stimulation. The cumulative tension time integral (TTI) of each group is presented as mean ± SE and represents the total amount of contractile work performed over the duration of the entire time course.

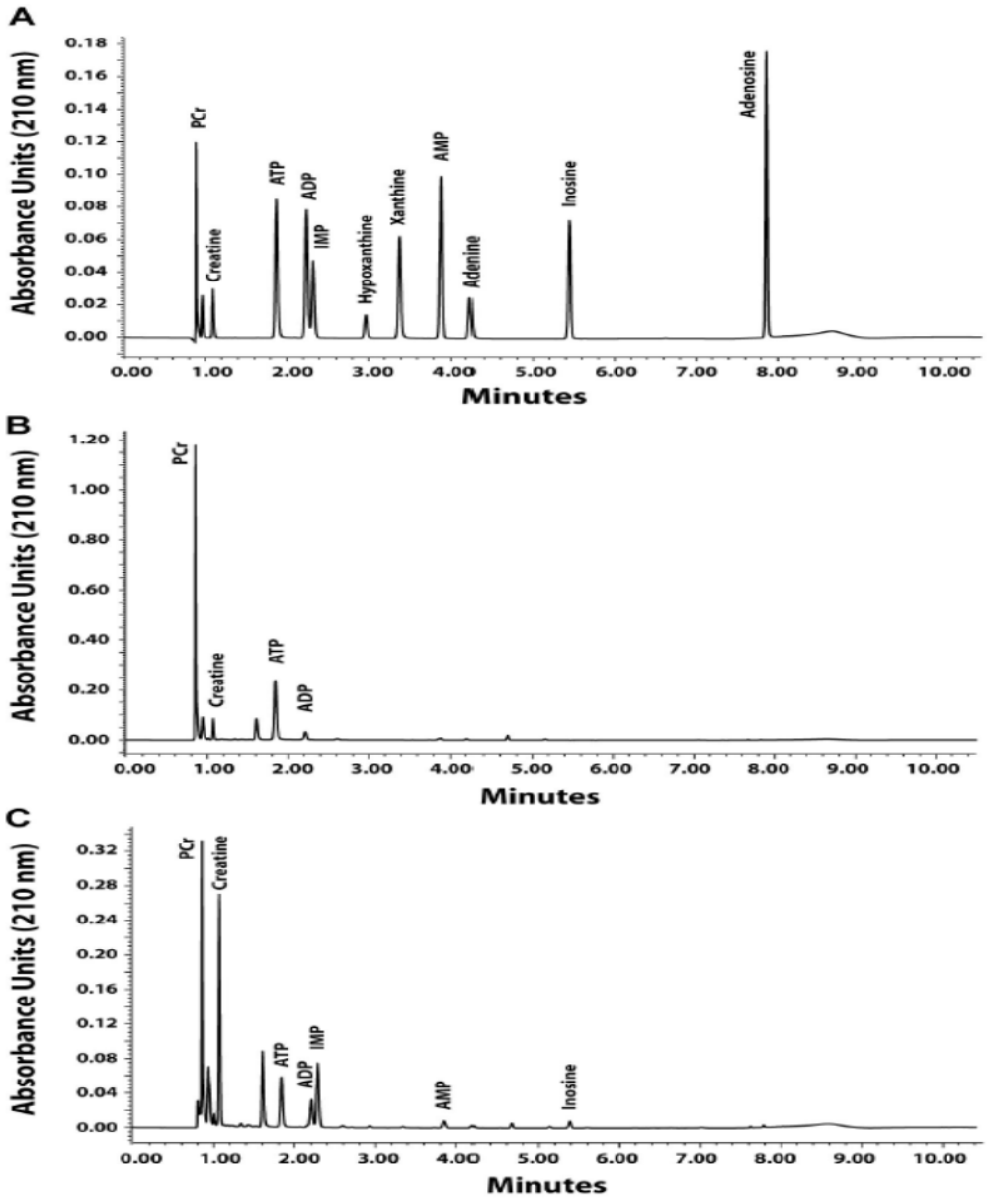

Figure 6. Ultra-Performance Liquid Chromatography Chromatograms. A: Chromatogram of a standard mixture containing 100pmol each phosphocreatine (PCr), creatine, ATP, ADP, AMP, IMP, adenosine, inosine, and xanthine and 25pmol each hypoxanthine and adenine. B: Chromatogram of a perchloric acid extract of a non-contracted EDL muscle incubated at resting length. Injection volume was 2 µl were used with detection limits of 0.2 pmol. C: Chromatogram of an extract from an EDL muscle after contracting at 10 Hz for 15 min.

Table II. Treatment Effects on Metabolites During Fatigue Protocol. Phosphocreatine (PCr), creatine (Cr), adenine nucleotide, inosine monophosphate (IMP) and inosine content of resting (Non-Stimulated) and 15 minute stimulated (Control, BTS, CPA, and BTS+CPA) EDL Muscles.

	PCr	Creatine	[PCr]/[Cr]	ATP	ADP	AMP	IMP	Inosine
Non-stimulated	14.53 ± 0.76	5.05 ± 0.27	2.94 ± 0.25	4.24 ± 0.39	0.59 ± 0.03	0.16 ± 0.03	0.35 ± 0.09	0.11 ± 0.03
Control	3.89 ± 0.24*	13.84 ± 0.28*	0.28 ± 0.02*	1.15 ± 0.15*	0.61 ± 0.06	0.20 ± 0.01	2.48 ± 0.09*	0.25 ± 0.03*
BTS	4.58 ± 0.80*	13.16 ± 0.29*	0.35 ± 0.06*	1.97 ± 0.15*	0.66 ± 0.02	0.18 ± 0.01	1.90 ± 0.09*,**	0.16 ± 0.01
CPA	9.32 ± 0.86*,**	10.14 ± 0.56*,**	0.96 ± 0.14*,**	2.21 ± 0.21*,**	0.60 ± 0.02	0.14 ± 0.01	2.15 ± 0.21*,**	0.18 ± 0.03
BTS + CPA	11.84 ± 0.68**	7.33 ± 0.48*,**	1.68 ± 0.18*,**	3.61 ± 0.18**	0.68 ± 0.04	0.15 ± 0.03	0.58 ± 0.08**	0.07 ± 0.02**

Values expressed as μmol/g, mean ± SE.
*Significantly different ($P < 0.05$) than non-stimulated.
**Significantly different ($P < 0.05$) than control.

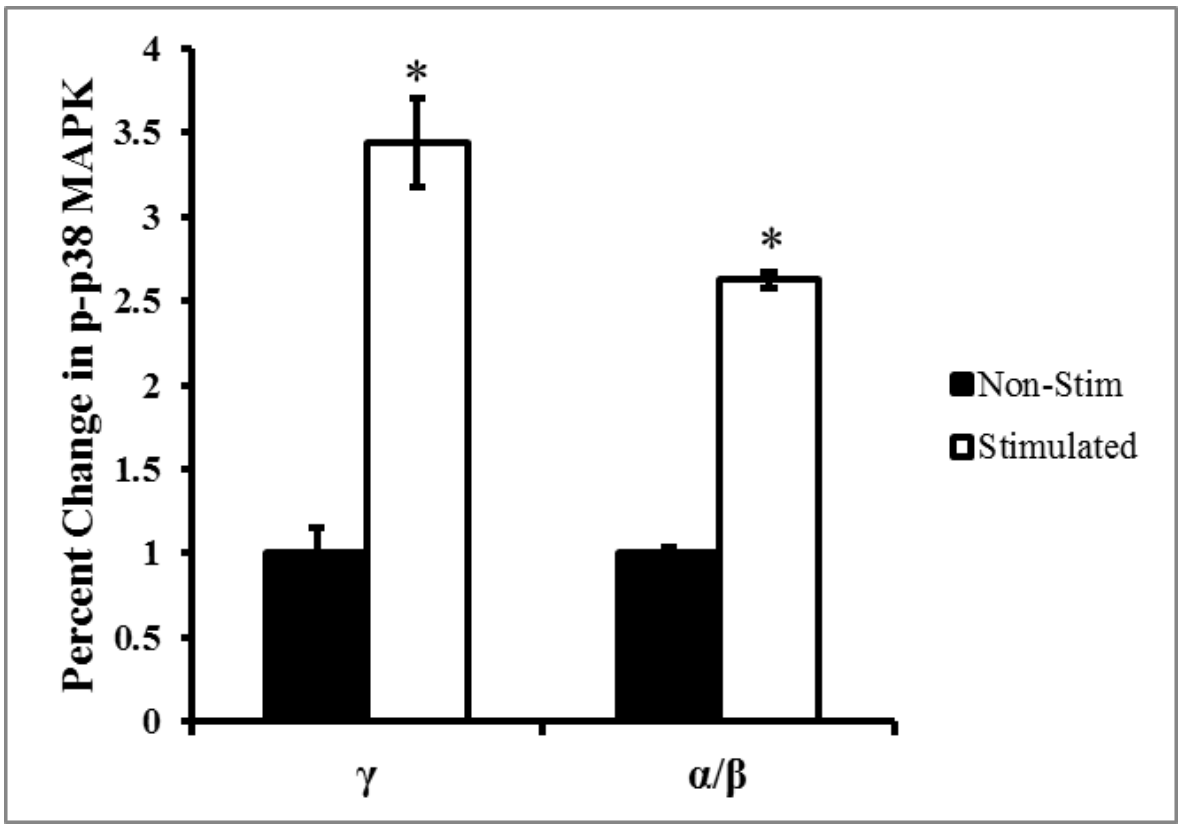

Figure 7. Phosphorylation Change of the MAPK Isoforms During Rest and Stimulation. EDLs were either stimulated at 10 Hz at 15 minutes (Stimulated) or non-stimulated (Non-Stim) for 15 minutes. Protein levels of phospho-p38 MAPK isoforms were determined by western blot. Quantification was based on the percent increase in the phosphorylated protein relative to the control phosphorylation intensities detected by Western blot analysis (n=3). There is a significant increase seen in phosphorylation of each of the p38-MAPK isoforms in skeletal muscle that received electrical stimulation. Bar graphs represent the mean ± SE; n=3 (p38γ MAPK $p=0.001$; p38α/β MAPK $p=6.4x10^{-5}$).

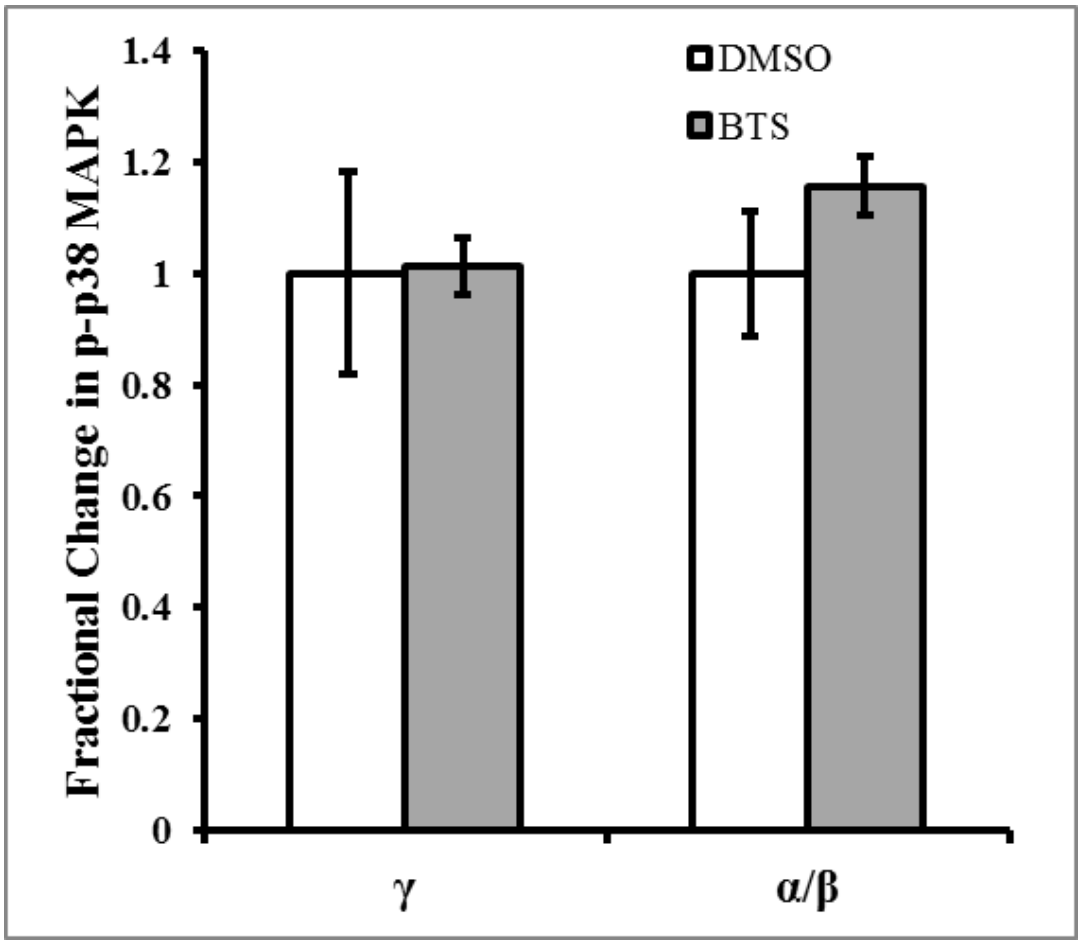

Figure 8. Phosphorylation Change of the MAPK Isoforms During Stimulation with DMSO or BTS Treatment. Muscles were treated without (DMSO) or with (BTS) cytosolic actinomyosin ATPase inhibitor and then stimulated for 15 minutes at 10 Hz. Protein levels of phospho-p38 MAPK isoforms were determined by western blot. Quantification was based change in band intensity of phosphorylated protein relative to the control phosphorylated protein levels detected by Western blot analysis. Bar graphs represent the mean ± SE; n=4.

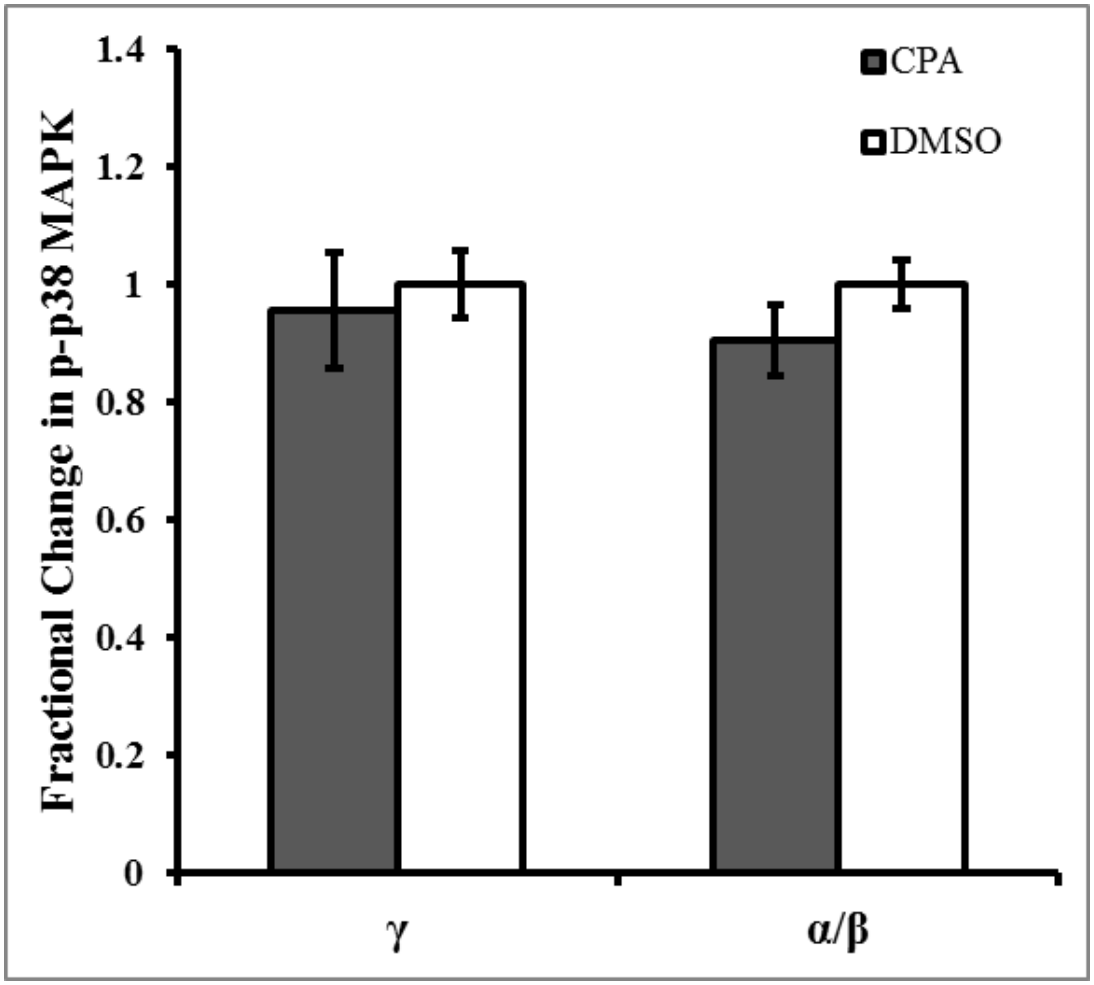

Figure 9. Phosphorylation Change of the MAPK Isoforms During Stimulation with DMSO or CPA Treatment. Muscles were treated without (control) or with (CPA) cytosolic SERCA ATPase inhibitor and then stimulated for 15 min at 10 Hz. Protein levels of phospho-p38 MAPK isoforms were determined by western blot. Quantification was based on the change in the band intensity of treated phosphorylated protein relative to the control phosphorylated levels detected by Western blot analysis. Bar graphs represent the mean ± SE; n=4.

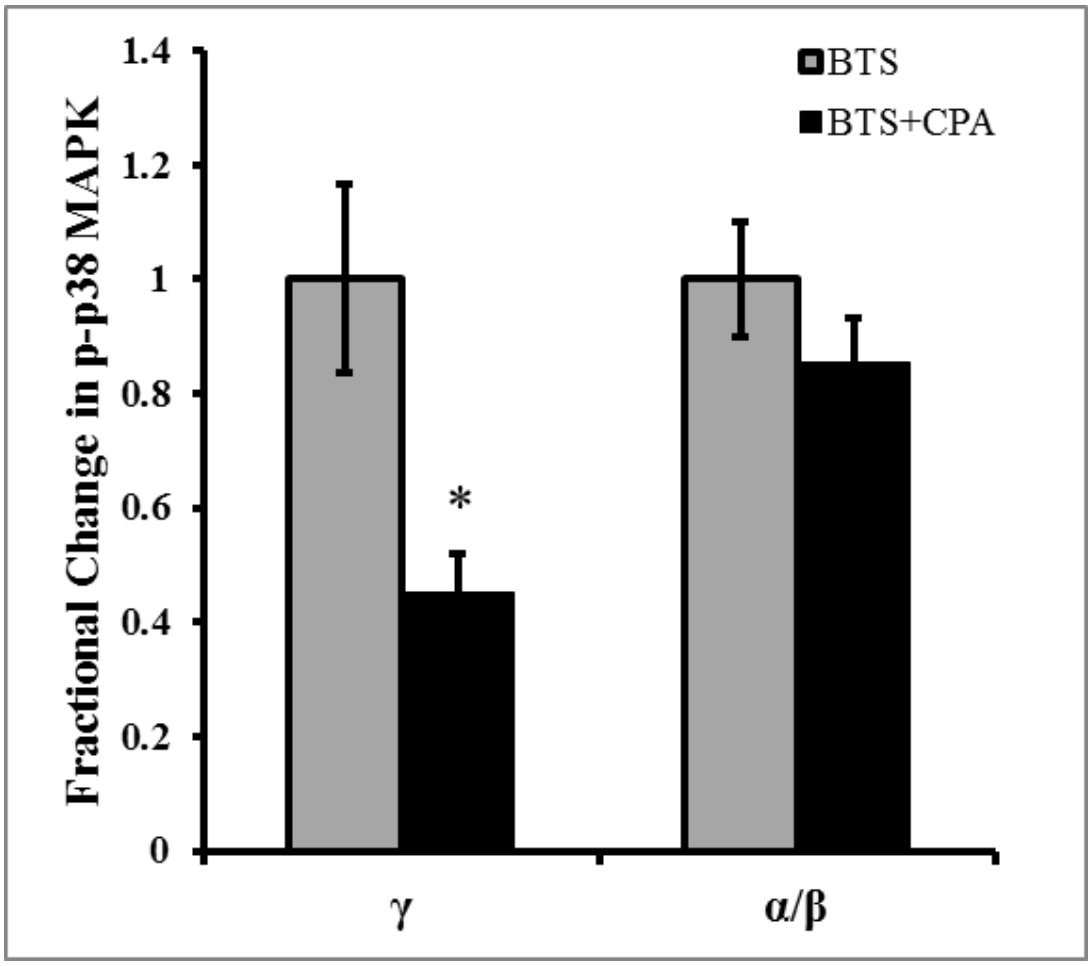

Figure 10. Phosphorylation Change of the MAPK Isoforms During Stimulation with BTS or BTS+CPA Treatment. Muscles were treated with BTS or BTS+CPA in combination (actinomyosin ATPase or SERCA ATPase inhibitor) and then stimulated for 15 min at 10 Hz. Protein levels of phospho-p38 MAPK isoforms were determined by western blot. Quantification was based on the change in the band intensity of the treated phosphorylated protein relative to BTS treated intensity levels detected by western blot analysis. Bar graphs represent the mean ± SE; n=4 (p38γ MAPK p=0.048; p38α/β MAPK p=0.24).

Specific Aim II: Inhibition of AMPK

A compound c dose response curve was created for incubation of *ex* vivo mouse skeletal muscle. EDL muscles were incubated with increasing concentrations of compound c at 80, 100, 120 and 140μM for 60 minutes prior to stimulation at 2 Hz for 20 minutes with a 2 ms pulse duration (Figure 2B) (stimulation protocol (Funai & Cartee 2009). Comparable amounts of DMSO were added for controls. This decrease in frequency of stimulation was done to ensure the fast twitch fibers of the EDL were not mechanically damaged with the higher stimulation protocols used in the previous study. Quantification of western blots seems to trend toward a decrease in AMPK phosphorylation with concentration of 120 and 140 μM (Figure 11). However, p-ACC western intensities show no change in the activity of AMPK, even with the decrease seen in the phosphorylation status of AMPK at the higher concentrations of compound c (n=2) (Figure 12). Increasing concentrations of compound c incubation prior to stimulation appeared to have no effect on the activation state of p38γ MAPK in comparison to DMSO treated muscles prior to stimulation (n=1; data not shown).

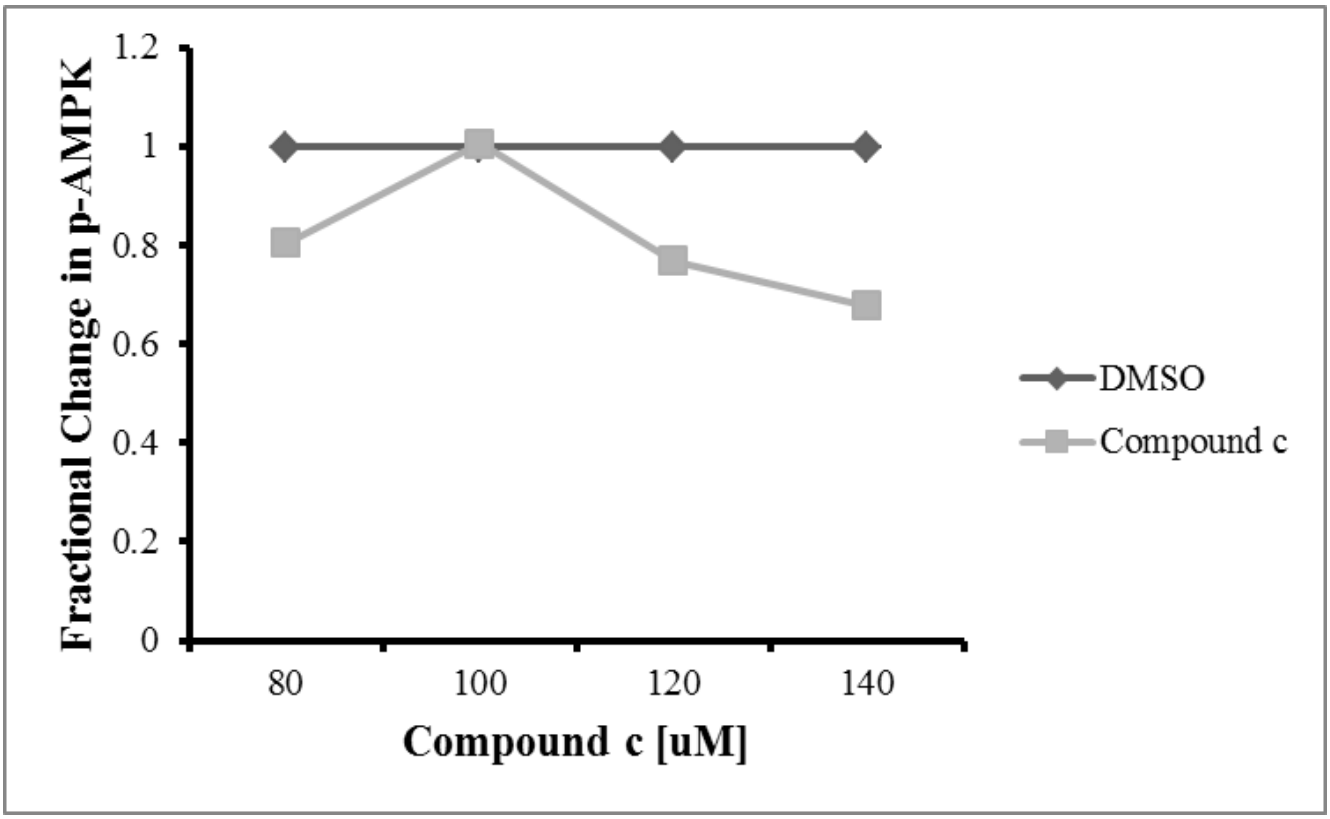

Figure 11. Compound C Dose Response Curve Effects on the Phosphorylation of AMPK.

Dose response curve for compound c with increasing concentrations at 80, 100, 120 and 140µM incubated for 60 minutes before stimulation at 10 Hz for 15 minutes. Western blot band intensities of p-AMPK were normalized to the percent change in phosphorylation from DMSO incubated muscles; n=2.

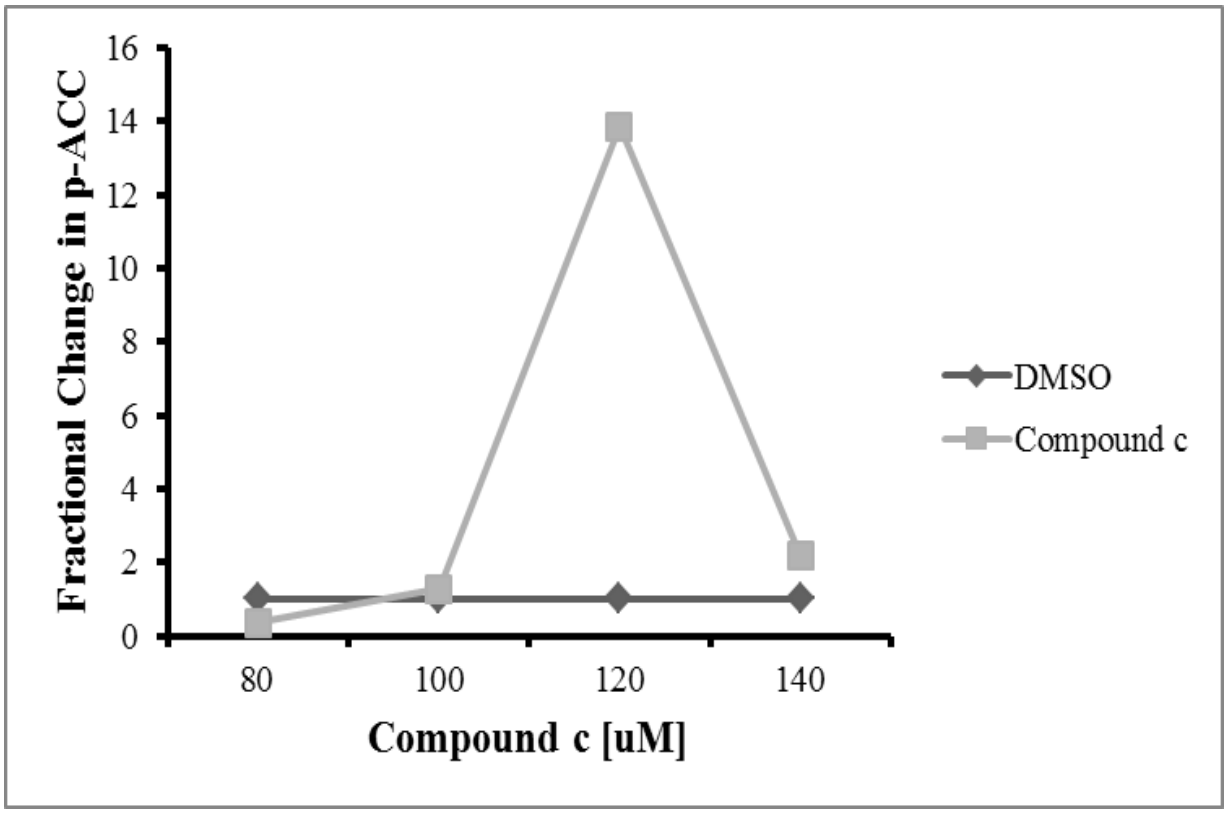

Figure 12. Compound C Dose Response Curve Effects on the Phosphorylation of ACC.

Dose response curve for compound c with increasing concentrations at 80, 100, 120 and 140µM incubated for 60 minutes before stimulation at 10 Hz for 15 minutes. Western blot quantification was done by percent change of band intensities in comparison to DMSO treated muscles; n=2.

Specific Aim III: Synthetic Activation of AMPK

Since compound c is unable to inhibit AMPK activity in mouse skeletal muscle (Fujii et al. 2006), synthetic activation of AMPK during rest allows the isolation of AMPK phosphorylation from energetic demand to look at its downstream effects. The synthetic activator, AICAR was used to measure the phosphorylation state of p38γ MAPK in comparison to control. The baseline was monitored to ensure AICAR did not cause a change in the tension of the EDLs and a twitch was administered every 30 minutes to ensure the viability of the muscle (Figure 2C). After 2 hours of AICAR incubation, there was a significant increase in AMPK phosphorylation (Figure 13) and in phosphorylation of ACC (Figure 14), a downstream target of AMPK, in comparison to phosphorylation levels of muscles treated with DMSO (control). At the end of the 2 hour AICAR incubation, there was a slight increase in the phosphorylation/activation state of p38γ MAPK in comparison to resting controls, but did not reach significance (Figure 15).

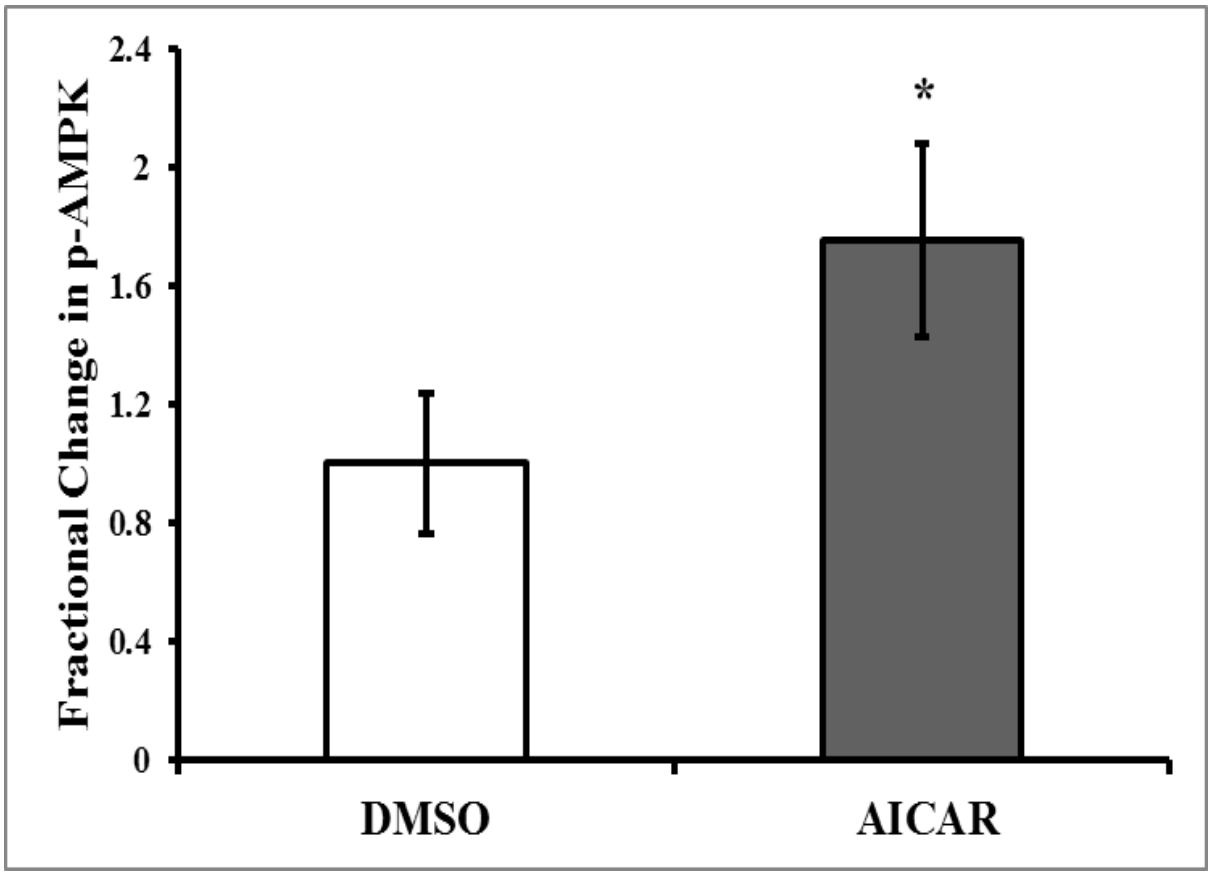

Figure 13. Effects of AICAR on the Phosphorylation of AMPK. EDL muscles hung at resting length were treated with 2mM AICAR for 2 hours; the baseline was monitored and a twitch administered every 30 minutes in order to ensure the viability of the muscles. Protein levels of p-AMPK are shown which were determined by western blot and quantified by the percent change in the intensity of AICAR in comparison to DMSO. Bar graphs represent the mean ± SE; n=16 (p=0.035).

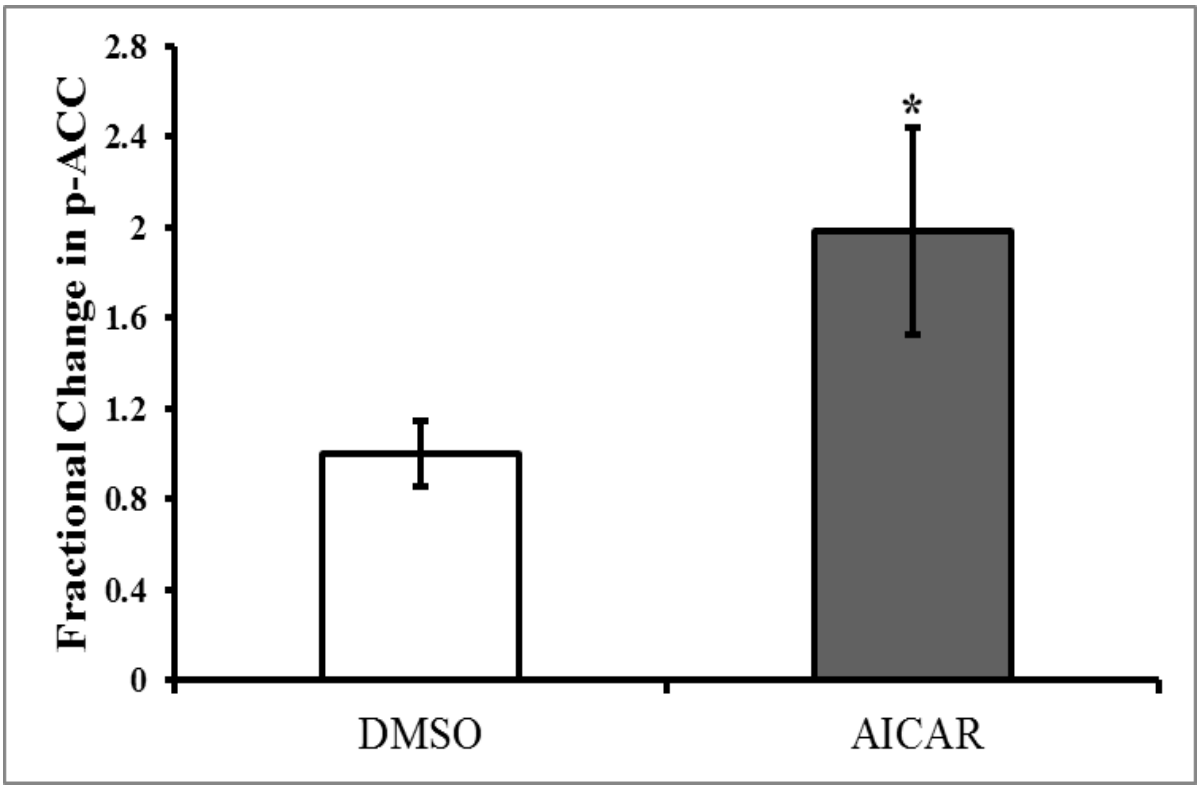

Figure 14. Effects of AICAR on the Phosphorylation of ACC. EDL muscles hung at resting length were treated with 2mM AICAR for 2 hours. The baseline was monitored and a twitch administered every 30 minutes in order to ensure the viability of the muscles. The percent change in p-ACC is shown, which was determined by quantification of western blot comparing control (DMSO) to AICAR treatment. Bar graphs represent the mean ± SE; n=11 (p=0.026).

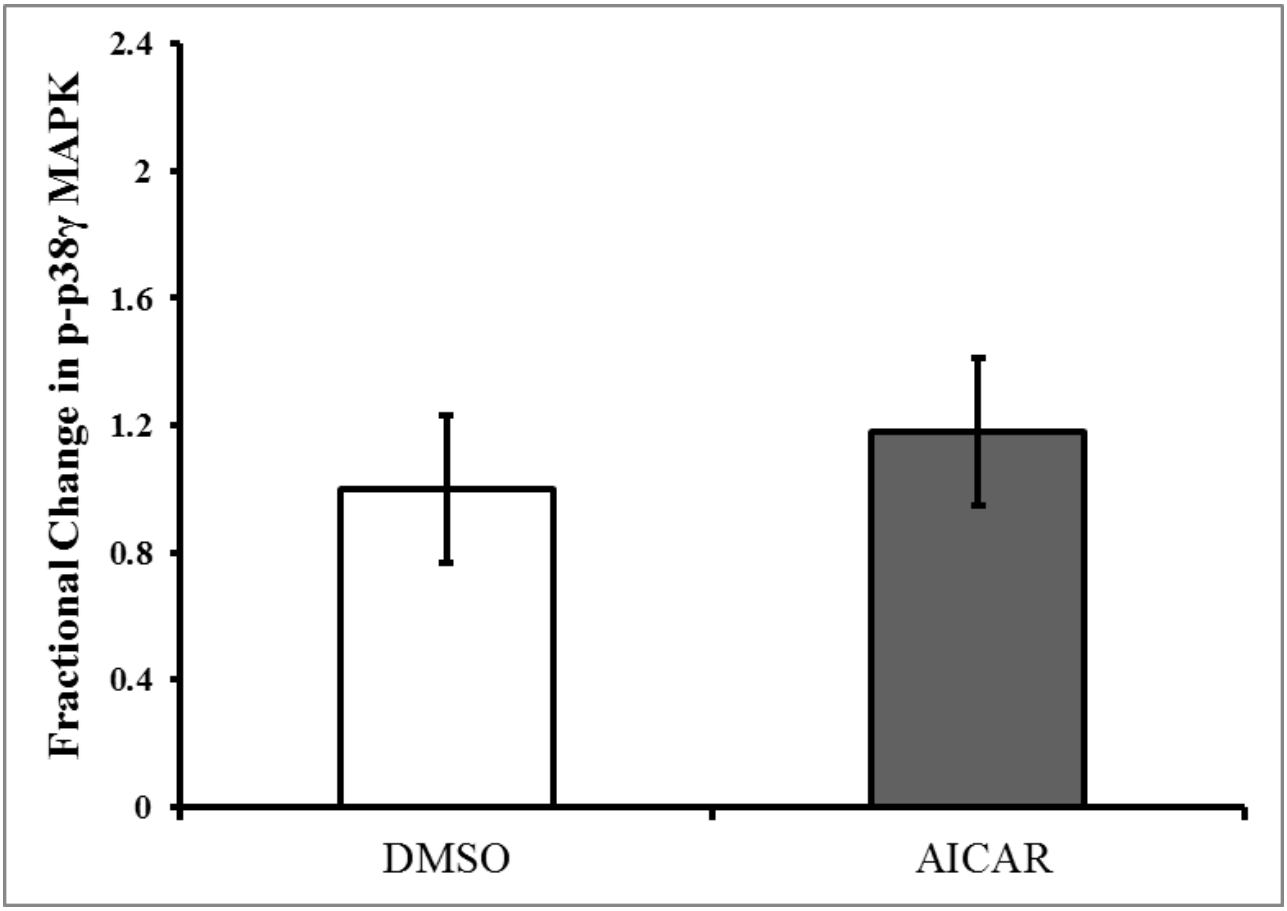

Figure 15. Effects of AICAR on the Phosphorylation of p38γ MAPK. EDL muscles hung at resting length were treated with 2mM AICAR for 2 hours. The baseline was monitored and a twitch administered every 30 minutes in order to ensure the viability of the muscles. Protein levels of p-p38γ MAPK are shown which were determined by western blot quantification comparing the percent change in intensity between the control (DMSO) and AICAR treated muscles. Bar graphs represent the mean ± SE; n=15 (p=0.320).

Specific Aim IV: Isolation of Energetic Drain

Since there was no significant increase in phosphorylation of p38γ MAPK, it is possible that energetic demand or a component of it is sufficient to increase activation of p38γ MAPK. In order to isolate energetic drain, without any other physiological factors, 2-deoxyglucose (DG) was used. When DG is introduced it is phosphorylated into 2-deoxyglucose 6-phosphate which is not further metabolized causing inhibition of glycolysis (Bachelard et al. 1971). This should cause energetic drain in the cell with no other physiological effects that normally occur during exercise. Levels of p-AMPK were measured after incubation with 20mM DG for 40 minutes using quantification of Western Blots (Figure 16). There was no percent change in the intensity of the bands in comparison to control levels (Figure 17). Phosphorylated p38γ MAPK band intensities were also measured, but also showed no change when compared to control.

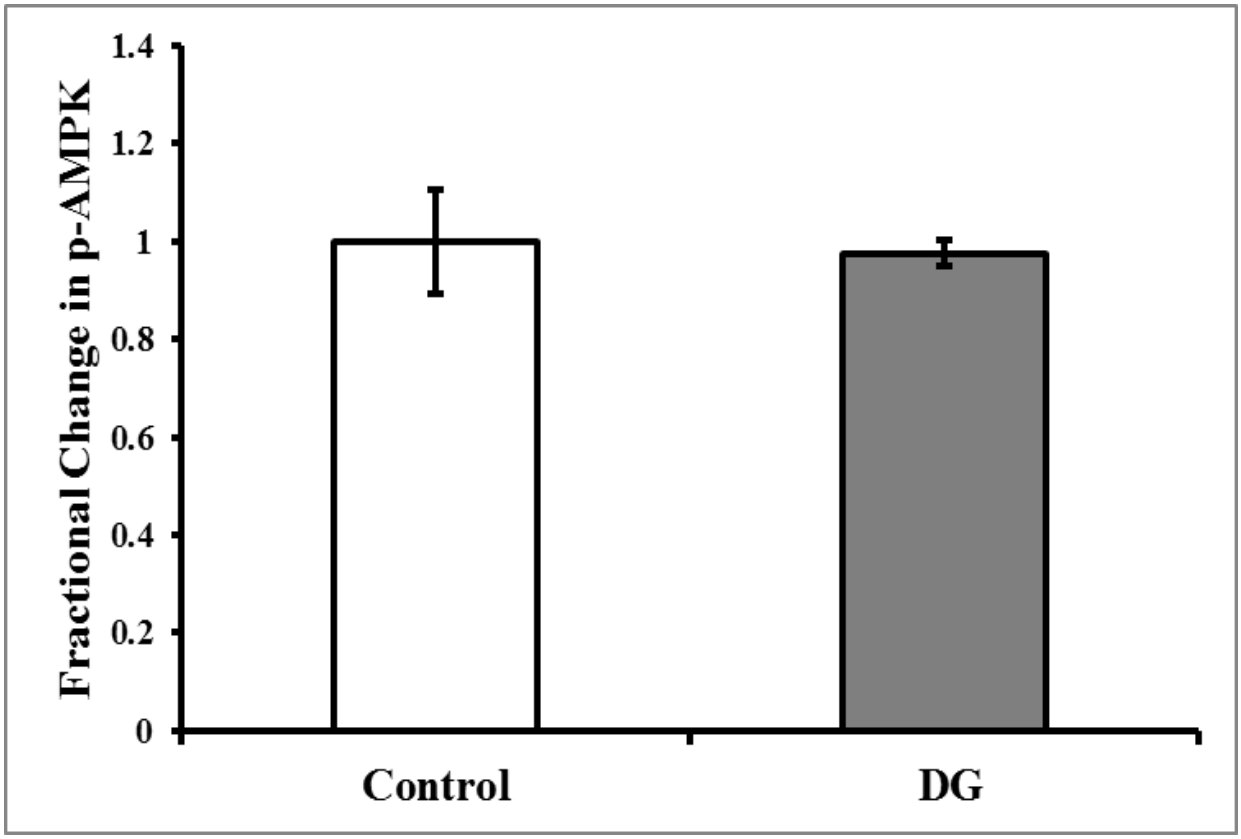

Figure 16. Effects of 2-Deoxyglucose on the Phosphorylation of AMPK. EDL muscles were hung at resting length and incubated with either DMSO (control) or 20mM 2-deoxyglucose (DG). Phospho-AMPK Western blot quantification was done through comparing the percent change of the band intensities between the control muscles and those treated with DG. There was no change in the band intensities when comparing the two groups. Bar graphs represent the mean ± SE; n=4 (p=0.44).

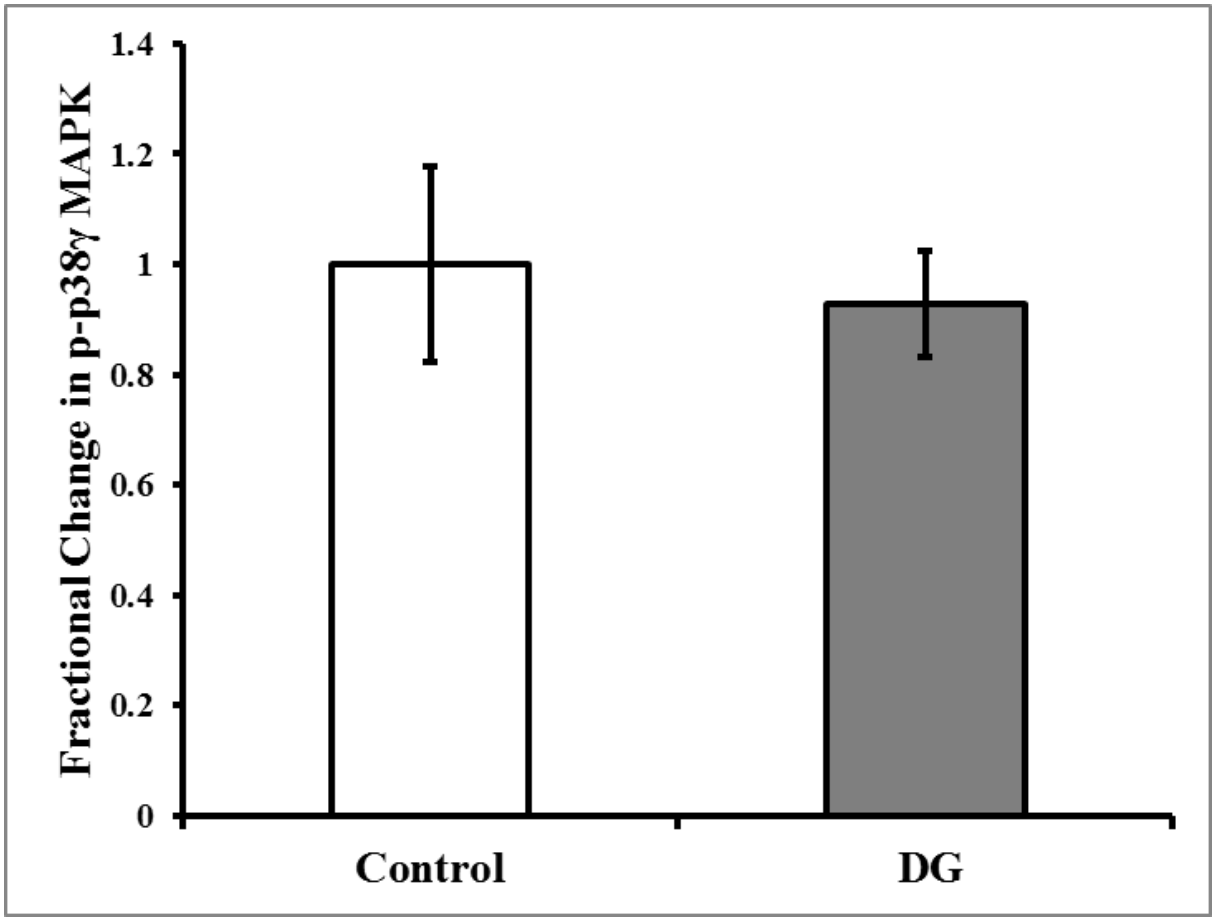

Figure 17. Effects of 2-Deoxyglucose on the Phosphorylation of p38γ MAPK. EDL muscles were hung at resting length and incubated with either DMSO (control) or 20mM 2-deoxyglucose (DG). Western blot quantification was done through comparing the percent change of the band intensities between the control muscles and those treated with DG. There was no change in the band intensities when comparing the intensities of p-p38γ MAPK between the two treatment groups. Bar graphs represent the mean ± SE; n=7 (p=0.40).

DISCUSSION

Exercise leads to beneficial adaptation throughout the entire body. One of these adaptations is an increase in aerobic capacity through mitochondrial biogenesis. PGC-1α has been identified as a biogenesis marker (Wu et al. 1999) and two of the transduction pathways correlated with its activation are AMPK and p38 MAPK (Pogozelski et al. 2009; Winder et al. 2013; Jäger et al. 2007). These kinases were isolated in order to increase the understanding of the signaling pathway leading to mitochondrial biogenesis.

Activation of p38γ MAPK has a specific role in mitochondrial biogenesis shown by Pogozelski et al with the p38 MAPK isoform specific knockout mice. In this study they show with 4 weeks of voluntary running there is an increase in mitochondrial content in the α/β specific isoform knockout models, but not the p38γ knockout. This identifies p38γ MAPK as the specific isoform necessary for mitochondrial biogenesis to occur after exercise (Pogozelski et al. 2009). Through the inhibition of the two major ATPases in skeletal muscle, the physiological activation mechanism during stimulation of the p38 MAPKs was examined. These data confirm that in stimulated muscles when compared to resting, hanging controls there is a 2.6-fold increase in the phosphorylation of the α/β isoforms and a 3.4-fold increase in phosphorylation of γ MAPK (Figure 7). BTS treatment alone shows with the inhibition of the actinomyosin ATPase, there is no change in the activation state of any of the MAPK's suggesting that force production is not the mechanism of activation (Figure 8). CPA alone causes inhibition of SERCA resulting in calcium flooding the cytoplasm inducing potentiation of force (Figure 9). However there is no change in the phosphorylation state of the p38 isoforms in comparison to control stimulation. This demonstrates that neither the sustained cytosolic Ca^{2+} levels nor the reduction of energetic

demands associated with calcium pumping were sufficient to alter the phosphorylation pattern for any of the p38 isoforms.

When BTS and CPA are combined there is inhibition of the two major ATPase, which are responsible for about 90% of the energetic demand during electrical stimulation. Only with combined treatment is activation of p38γ MAPK specifically blunted by 2.5 fold, suggesting that the energetic demand is responsible for its phosphorylation (Figure 10). Combined treatment does not alter the activation state of p38α and β MAPK. These data suggest that the change in energetics is what induces phosphorylation of p38γ alone, while another physiological component of exercise is responsible for the activation of the p38α and β isoforms.

AMPK is an energy sensing kinase and is activated during exercise (Hardie et al. 1998). Since energetic drain is what leads to the activation of p38γ MAPK, it was speculated that AMPK could be responsible for its activation. If there is decreased activation/phosphorylation of AMPK with compound c incubation prior to stimulation and blunted phosphorylation of p38γ MAPK, it would suggest that AMPK is sufficient for activation of p38γ MAPK. A dose response curve was created to find the optimal concentration of compound c to inhibit AMPK activity during stimulation. Increasing concentrations of compound c during stimulation seem to slightly decrease the phosphorylation of AMPK. However, unaltered phosphorylation of downstream ACC, suggests that compound c is insufficient to blunt the activity of AMPK. Fujii et al states that compound c does not work in the mouse skeletal muscle (Fujii et al. 2006). Therefore, this is not a suitable mechanism in mice to test the hypothesis that AMPK is an upstream activator of p38γ MAPK.

AICAR can synthetically lead to activation of AMPK via ZMP, and cause downstream phosphorylation of ACC (Corton et al. 1995). Using AICAR would show in resting muscle that AMPK is sufficient to activate/phosphorylate p38γ MAPK. AICAR would isolate AMPK phosphorylation and allow a further understanding of its downstream effects. Phosphorylation of p38γ MAPK does not show a significant increase after incubation of AICAR for 2 hours, suggesting that AMPK phosphorylation/activation is not sufficient to induce activation of the p38γ MAPK isoform (Figure 15). Therefore, these findings suggest that a component of energetic demand alone could lead to the activation of p38γ MAPK.

Since AMPK was insufficient to significantly increase the phosphorylation of p38γ MAPK, isolation of energetic drain could allow further understanding of the activation mechanisms. 2-Deoxyglucose (DG) is a glucose molecule that has the normal 2-hydroxyl group replaced by hydrogen. DG acts as a competitive inhibitor of glycolysis through the enzyme hexokinase and forms the product glucose-6-phosphate (Bachelard et al. 1971). This buildup of glucose-6-phosphate, through the inhibition of glycolysis, causes an increase in the AMP: ATP. Incubation with DG would show that a change in energetics, without any other contributing factors, can lead to activation of p38γ MAPK independently of AMPK activation. If both are activated by a change in energetics, then both should be phosphorylated/ activated with DG incubation. Western blot quantification shows that there is no change in the phosphorylation state of neither AMPK nor p38γ MAPK (Figure 16 and Figure 17). These data may suggest that another physiological factor is responsible for their activation. More likely it could be due to an insufficient drain of energetics to cause activation of either of the kinases.

Cuthbertson et al wanted to determine whether AICAR stimulates muscle glucose uptake in healthy males. They used DG as their measure of glucose uptake, and interestingly, with 180

minutes of DG infusion via the forearm vein, there was no change in the phosphorylation of AMPK or ACC (Cuthbertson et al. 2007). This result correlates with the data presented here, revealing no change in the phosphorylation level of AMPK or p38γ MAPK with DG incubation. DG could be an insufficient mechanism of inducing energetic drain in resting skeletal muscle. Therefore, another mechanism to isolate energetic stress may show more precisely its role in the activation of the kinases.

A recent study shows that AMPK may not be activated directly by an increase in the AMP: ATP ratio, but via an indirect mechanism through liver kinase B1 (LKB1) (Tanner et al. 2013). Tanner et al show through a LKB1 skeletal muscle specific knock out that AMPK activation is dependent on LKB1. There is no increase in the phosphorylation of AMPK in the skeletal muscle specific knockout model in comparison to the control when incubated with AICAR or in hind limb electrical stimulation.

The p38 MAPKs could be activated by an indirect component of energetic drain. XO activity increases with energetic drain. Inosine, a component of fatigue is further broken down into hypoxanthine and ribose. When there are increasing levels of hypoxanthine, xanthine oxidase levels increase and produce reactive oxygen species (Nivorozhkin & Szabo 2006). In a recent study by Wadley et al, they show a correlation to p38 MAPK activation xanthine oxidase (XO) inhibition. This study uses an inhibitor of XO, allopurinol, which causes a decrease in the activation of p38 MAPK; this study does not look at the specific isoforms in skeletal muscle (Wadley et al. 2013). XO is located in the endothelium of the skeletal muscle (Jackson 2011). It could be possible that XO, or a product of XO activity, is responsible for the activation of p38γ MAPK and in turn for mitochondrial biogenesis. It could also be possible that it is responsible

for the activation of α and β isoforms. Further experiments need to be done in order to understand the exact mechanisms of activation.

Results from Brault et al. and the AICAR studies suggest that p38γ MAPK is activated by a change in energetics but not via AMPK (Brault et al. 2013). Still, it is unknown whether p38γ MAPK can be activated directly by the change in energetics or indirectly via another upstream kinase. It is also unknown which element of the change in energetics is responsible. If DG did not create an energetic drain sufficient to activate p38γ MAPK, another component of energetic drain maybe required.

PGC-1α has been suggested to be activated by both AMPK and p38 MAPK (Chin 2004; Pogozelski et al. 2009; Winder et al. 2013). Their mechanism of activation and role in this transcription factor activation for mitochondrial biogenesis has yet to be identified. These studies done do not determine whether either or both kinases are able to activate PGC-1α. Further experiments need to be done in order to see which is responsible for the translocation of PGC-1α. This study shows that both AMPK and p38γ MAPK are downstream of a change in the energetic signal, yet which plays a pivotal role in the signaling pathway of mitochondrial biogenesis is still unknown. This study does confirm that both AMPK and p38γ MAPK are activated with electrical stimulation in skeletal muscle and suggests that AMPK is insufficient to significantly activate p38γ MAPK. Further experiments would need to be done to better understand the signaling pathway leading to mitochondrial biogenesis.

CONTINUED RESEARCH

- 2-deoxyglucose incubation revealed no change in the activation states of either AMPK or p38γ MAPK. Nuclear magnetic spectroscopy would measure the change in energetics during incubation. This would determine whether there was energetic drain and provide a better understanding why it was insufficient to induce activation.
- LKB1 has been shown to be an upstream activator of AMPK (Tanner et al. 2013). Measurements of LKB1 could be taken in order to ensure its activation with AICAR and energetic stimulation. An LKB1 inhibitor could be used to see if it is possibly an activator of p38γ MAPK. LKB1 could be upstream of both AMPK and p38γ MAPK; LKB1 is activated by a change in energetics and could be responsible for the activation of both kinases.
- XO could have a specific correlation with one or all of the isoforms of MAPK present in skeletal muscle. Conducting a similar study to that of Wadley et al, would provide a further understanding of the mechanisms of activation of the p38 MAPKs. Using the same antibodies as in the study above that binds to specific isoforms of p38 MAPK would specify which of the isoforms are activated through XO. Incubating muscles with allopurinol, an inhibitor of XO, prior to stimulation will identify if XO is responsible for the activation of p38γ MAPK and mitochondrial biogenesis.
- Nuclear measurements of PGC-1α would need to be taken in order to confirm that both AMPK and p38γ MAPK play a role in the nuclear translocation of PGC-1α. The AICAR studies would show that AMPK can independently cause translocation of PGC-1α, if there was an increase in the nuclear levels. This would show that p38γ MAPK is not necessary for the activation and translocation of PGC-1α and that AMPK is sufficient for

initiation of mitochondrial biogenesis. If there is not a significant increase in the translocation of PGC-1α with AICAR incubation, then DOG experiments should be performed to see if energetics can lead to activation of p38γ MAPK and then measure the nuclear levels of PGC-1α. This would show that p38γ MAPK is necessary for the translocation of PGC-1α and initiation of mitochondrial biogenesis.

- Lastly, with the theory that there is a mitochondrial defect in diabetes (REF), it would be beneficial to look at the protein levels of both AMPK and p38 MAPK in a diabetic model. This would look at their levels both in a resting muscle and in a stimulated muscle to see if there are changes in both the protein content and the activity levels. This would help us to better understand the signaling mechanisms in the disease state and increase of understanding in the changes that occur with the mitochondria in the skeletal muscle.

BIBLIOGRAPHY

BIBLIOGRAPHY

Akimoto, T., Pohnert, S.C., Li, P., Zhang, M., Gumbs, C., Rosenberg, P.B., Williams, R.S., & Yan, Z., 2005. Exercise stimulates Pgc-1alpha transcription in skeletal muscle through activation of the p38 MAPK pathway. *The Journal of Biological Chemistry*, 280(20), 19587–19593.

Bachelard, B.H.S., Clark, A.G. & Thompson, M.F., 1971. Cerebral-Cortex Hexokinases. Elucidation of reaction mechanisms by substrate and dead-end inhibitor kinetic analysis. *The Biochemical Journal*, 123(5), 707-715

Bassel-Duby, R. & Olson, E.N., 2006. Signaling pathways in skeletal muscle remodeling. *Annual review of biochemistry*, 75, pp.19–37.

Baudet, S., Shaoulian, R. & Bers, D.M., 1993. Effects of thapsigargin and cyclopiazonic acid on twitch force and sarcoplasmic reticulum Ca2+ content of rabbit ventricular muscle. *Circulation Research*, 73(5), 813–819.

Booth, F.W., Chakravarthy, M. V & Spangenburg, E.E., 2002. Exercise and gene expression: physiological regulation of the human genome through physical activity. *The Journal of Physiology*, 543(2), 399–411.

Brault, J.J., Pizzimenti, N.M., Dentel, J.N., & Wiseman, R.W., 2013. Selective inhibition of ATPase activity during contraction alters the activation of p38 MAP kinase isoforms in skeletal muscle. *Journal of cellular biochemistry*, 1455, 1445–1455.

Cheung, A., Dantzig, J., Hollingworth, S., Baylor, S., Goldman, Y., Mitchison, T., & Straight, A., 2002. A small-molecule inhibitor of skeletal muscle myosin II. *Nature Cell Biology*, 4(1), 83-88.

Chin, E.R., 2004. The role of calcium and calcium/calmodulin-dependent kinases in skeletal muscle plasticity and mitochondrial biogenesis. *The Proceedings of the Nutrition Society*, 63(2), 279–86.

Corton, J.M., Gillespie, J.G., Hawley, S.A., & Hardie, D.G., 1995. 5-Aminoimidazole-4-carboxamide ribonucleoside A specific method for activating AMP-activated protein kinase in intact cells? *European Journal of Biochemistry*, 565, 558–565.

Crow, M.T. & Kushmerick, M.J., 1982. Chemical energetics of slow- and fast-twitch muscles of the mouse. *The Journal of general physiology*, 79(1), 147–66.

Csukly, K.J., Martineau, L.C. & Gardiner, P.F., 2002. Inter- and intra-muscle comparisons of MAPK mechanosensitivity: evidence for the absence of fibre-type dependency. *Pflügers Archiv : European journal of physiology*, 444(6), 732–7.

Cuadrado, A. & Nebreda, A.R., 2010. Mechanisms and functions of p38 MAPK signalling. *The Biochemical journal*, 429(3), 403–17.

Cuenda, A. & Rousseau, S., 2007. p38 MAP-kinases pathway regulation, function and role in human diseases. *Biochimica et biophysica acta*, 1773(8), 1358–75.

Cuthbertson, D.J., Babraj, J.A., Mustard, K.J.W., Towler, M.C., Green, K.A., Wackerhage, H., Leese, G.P., Baar, K., Thomason-Hughes, M., Sutherland, C., Hardie, D.G., & Rennie, M.J., et al., 2007. 5-aminoimidazole-4-carboxamide 1-beta-D-ribofuranoside acutely stimulates skeletal muscle 2-deoxyglucose uptake in healthy men. *Diabetes*, 56(8), 2078-2084.

Dentel, J.N., Blanchard, S.G., Ankrapp, D.P., McCabe, L.R., & Wiseman, R.W., 2005. Inhibition of cross-bridge formation has no effect on contraction-associated phosphorylation of p38 MAPK in mouse skeletal muscle. *American journal of physiology Cell physiology*, 288(4), C824–C830.

McNally, E.M., Lapidos, K.A., & Wheeler, M.T., 2006. 67 Skeletal Muscle Structure and Function. In *Principles of Molecular Medicine*, 674–681.

Enslen, H., Brancho, D.M. & Davis, R.J., 2000. Molecular determinants that mediate selective activation of p38 MAP kinase isoforms. *The EMBO journal*, 19(6), 1301–11.

Frier, B.C., Wan, Z., Williams, D.B., Stefanson, A.L., & Wright, D.C., 2012. Epinephrine and AICAR-induced PGC-1α mRNA expression is intact in skeletal muscle from rats fed a high-fat diet. *American journal of physiology. Cell physiology*, 302(12), C1772–9.

Fuglevand, A. J., 2011. Mechanical properties and neural control of human hand motor units. *The Journal of Physiology*, 589(23), 5595–5602.

Fujii, N., Jessen, N. & Goodyear, L.J., 2006. AMP-activated protein kinase and the regulation of glucose transport. *American journal of physiology. Endocrinology and metabolism*, 291(5), E867–77.

Funai, K., & Cartee, G. D., 2009. Inhibition of contraction-stimulated AMP-activated protein kinase inhibits contraction-stimulated increases in PAS-TBC1D1 and glucose transport without altering PAS-AS160 in rat skeletal muscle. *Diabetes*, 58(5), 1096-1104.

Hancock, C.R., Janssen, E. & Terjung, R.L., 2005. Skeletal muscle contractile performance and ADP accumulation in adenylate kinase-deficient mice. *American journal of physiology. Cell physiology*, 288(6), C1287–97.

Hardie, D.G., Carling, D. & Carlson, M., 1998. The AMP-activated/SNF1 protein kinase subfamily: metabolic sensors of the eukaryotic cell? *Annual review of biochemistry*, 67, 821–55.

Heizmann, C.W., Berchtold, M.W. & Rowlerson, A.M., 1982. Correlation of parvalbumin concentration with relaxation speed in mammalian muscles. *Proceedings of the National Academy of Sciences of the United States of America*, 79(23), 7243–7.

Henneman, E. & Olson, C.B., 1965. Relations Between Structure and Function in the Design of Skeletal Muscles. *Journal of neurophysiology*, 28, 581–98.

Hoppeler, H. & Fluck, M., 2003. Plasticity of skeletal muscle mitochondria: structure and function. *Medicine and science in sports and exercise*, 35(1), 95–104.

Hu, M.C., Wang, Y.P., Mikhail, A., Qiu, W.R., & Tan, T.H., 1999. Murine p38-delta Mitogen-activated Protein Kinase, a Developmentally Regulated Protein Kinase That Is Activated by Stress and Proinflammatory Cytokines. *Journal of Biological Chemistry*, 274(11), 7095–7102.

Huang, C.L.-H., Pedersen, T.H. & Fraser, J.A., 2011. Reciprocal dihydropyridine and ryanodine receptor interactions in skeletal muscle activation. *Journal of muscle research and cell motility*, 32(3), 171–202.

Jackson, M.J., 2011. Control of reactive oxygen species production in contracting skeletal muscle. *Antioxidants & redox signaling*, 15(9), 2477–86.

Jäger, S., Handschin, C., St.-Pierre, J., & Spiegelman, B.M., 2007. AMP-activated protein kinase (AMPK) action in skeletal muscle via direct phosphorylation of PGC-1alpha. *Proceedings of the National Academy of Sciences of the United States of America*, 104(29), 12017–22.

Jørgensen, S.B., Viollet, B., Andreelli, F., Frøsig, C., Birk, J.B., Schjerling, P., Vaulont, S., Richter, E.A, & Wojtaszewski, J.F.P., 2004. Knockout of the alpha2 but not alpha1 5'-AMP-activated protein kinase isoform abolishes 5-aminoimidazole-4-carboxamide-1-beta-4-ribofuranosidebut not contraction-induced glucose uptake in skeletal muscle. *The Journal of biological chemistry*, 279(2), 1070–9.

Keesler, G. A., Bray, J., Hunt, J., Johnson, D. A., Gleason, T., Yao, Z., Wang, S. W., Parker, C., Yamane, H., Cole, C., & Lichenstein, H.S., 1998. Purification and activation of recombinant p38 isoforms alpha, beta, gamma, and delta. *Protein expression and purification*, 14(2), 221-228.

Kurebayashi, N., & Ogawa, Y., 1991. Discrimination of Ca2+-ATPase activity of the sarcoplasmic reticulum from actomyosin-type ATPase activity of myofibrils in skinned mammalian skeletal muscle fibres: distinct effects of cyclopiazonic acid on the two ATPase activities. *Journal of Muscle Research and Cell Motility*. 12, 355-365.

Kushmerick, M. J., Moerland, T. S., & Wiseman, R. W., 1992. Mammalian skeletal muscle fibers distinguished by contents of phosphocreatine, ATP, and Pi. *Proceedings of the National Academy of Sciences of the United States of America*, 89(16), 7521-7525.

Long, Y. C., & Zierath, J. R., 2006. AMP-activated protein kinase signaling in metabolic regulation. *The Journal of clinical investigation*, 116(7), 1776-1783.

MacIntosh, B.R., Holash, R.J. & Renaud, J.-M., 2012. Skeletal muscle fatigue--regulation of excitation-contraction coupling to avoid metabolic catastrophe. *Journal of cell science*, 125(Pt 9), 2105–14.

MacIntosh, B.R. & Shahi, M.R.S., 2011. A peripheral governor regulates muscle contraction. *Applied physiology, nutrition, and metabolism = Physiologie appliquée, nutrition et métabolisme*, 36(1), 1–11.

Mahlapuu, M., Johansson, C., Lindgren, K., Hjälm, G., Barnes, B.R., Krook, A., Zierath, J.R., Andersson, L., & Marklund, S., 2004. Expression profiling of the gamma-subunit isoforms of AMP-activated protein kinase suggests a major role for gamma3 in white skeletal muscle. *American journal of physiology. Endocrinology and metabolism*, 286(2), E194–200.

Même, W., Huchet-Cadiou, C., & Léoty, C. 1998. Cyclopiazonic acid-induced changes in the contraction and Ca2+ transient of frog fast-twitch skeletal muscle. *The American journal of physiology*, 274(1 Pt 1), C253-C261.

Morrison, D.K. & Davis, R.J., 2003. Regulation of MAP kinase signaling modules by scaffold proteins in mammals. *Annual review of cell and developmental biology*, 19, 91–118.

Ojuka, E.O., Jones, T.E., Han, D., Chen, M., & Holloszy, J.O., 2003. Raising Ca2+ in L6 myotubes mimics effects of exercise on mitochondrial biogenesis in muscle. *FASEB journal : official publication of the Federation of American Societies for Experimental Biology*, 17(6), 675–81.

Pogozelski, A.R., Geng, T., Li, P., Yin, X., Lira, V.A., Zhang, M., Chi, J., & Yan, Z., 2009. P38Gamma Mitogen-Activated Protein Kinase Is a Key Regulator in Skeletal Muscle Metabolic Adaptation in Mice. *PloS one*, 4(11), e7934.

Puigserver, P., Rhee, J., Lin, J., Wu, Z., Yoon, J.C., Zhang, C.Y., Krauss, S., Mootha, V.K., Lowell, B.B., & Spiegelman, B.M., 2001. Cytokine Stimulation of Energy Expenditure through p38 MAP Kinase Activation of PPAR γ Coactivator-1. *Molecular Cell*, 8(5), 971–982.

Rall, J.A, 2005. Energetics, mechanics and molecular engineering of calcium cycling in skeletal muscle. *Advances in experimental medicine and biology*, 565, 183–92; discussion 379–95.

Wiseman, R. W., & Kushmerick, M. J., 1995. Creatine kinase equilibration follows solution thermodynamics in skeletal muscle. 31P NMR studies using creatine analogs. *The Journal of biological chemistry*, 270(21), 12428-12438.

Robin, G., Berthier, C. & Allard, B., 2012. Sarcoplasmic reticulum Ca2+ permeation explored from the lumen side in mdx muscle fibers under voltage control. *The Journal of general physiology*, 139(3), 209–18.

Ryder, J.W., 2000. Effect of Contraction on Mitogen-activated Protein Kinase Signal Transduction in Skeletal Muscle. INVOLVEMENT OF THE MITOGEN- AND STRESS-ACTIVATED PROTEIN KINASE 1. *Journal of Biological Chemistry*, 275(2), 1457–1462.

Tanner, C.B., Madsen, S.R., Hallowell, D.M., Goring, D.M.J., Moore, T.M., Hardman, S.E., Heninger, M.R., Atwood, D.R., & Thomson, D.M., 2013. Mitochondrial and performance adaptations to exercise training in mice lacking skeletal muscle LKB1. *American journal of physiology. Endocrinology and metabolism*, 305(8), E1018-29.

Teerlink, T., Hennekes, M., Bussemaker, J., & Groeneveld, J., 1993. Simultaneous determination of creatine compounds and adenine nucleotides in myocardial tissue by high-performance liquid chromatography. *Analytical biochemistry*, 214(1), 278-283.

Vina, J. et al., 2012. Exercise acts as a drug; the pharmacological benefits of exercise. *British journal of pharmacology*, 167(1), 1–12.

Wadley, G.D. et al., 2013. Xanthine oxidase inhibition attenuates skeletal muscle signaling following acute exercise but does not impair mitochondrial adaptations to endurance training. *American journal of physiology. Endocrinology and metabolism*, 304(8), E853–62.

Wang, Y., 1998. Cardiac Muscle Cell Hypertrophy and Apoptosis Induced by Distinct Members of the p38 Mitogen-activated Protein Kinase Family. *Journal of Biological Chemistry*, 273(4), 2161–2168.

Winder, W. W., Holmes, B. F., Rubink, D. S., Jensen, E. B., Chen, M., & Holloszy, J. O., 2000. Activation of AMP-activated protein kinase increases mitochondrial enzymes in skeletal muscle. *Journal of applied physiology* (Bethesda, Md. : 1985), 88(6), 2219-2226.

Wu, Z., Puigserver, P., Andersson, U., Zhang, C., Adelmant, G., Mootha, V., Troy, A., Cinti, S., Lowell, B., Scarpulla, R.C., & Spiegelman, B.M., 1999. Mechanisms controlling mitochondrial biogenesis and respiration through the thermogenic coactivator PGC-1. *Cell*, 98(1), 115-124.

Young, I.S., Harwood, C.L. & Rome, L.C., 2003. Cross-bridge blocker BTS permits direct measurement of SR Ca2+ pump ATP utilization in toadfish swimbladder muscle fibers. *American journal of physiology. Cell physiology*, 285(4), C781–7.